Polymer Journal (2011) 43, 331–351

www.nature.com/pj

INVITED REVIEW

Living polymerization of olefins with *ansa*-dimethylsilylene(fluorenyl)(amido)dimethyltitanium-based catalysts

Takeshi Shiono

This article reviews the living homopolymerization and copolymerization of propene, 1-alkene and norbornene with *ansa*-dimethysilylene(fluorenyl)(amido)dimethyltitanium, $Me_2Si(\eta^3\text{-}C_{13}H_8)(\eta^1\text{-}N^tBu)TiMe_2$ and its derivatives, correlating the effects of cocatalysts, solvents, polymerization conditions and the substituents of the fluorenyl ligand with catalytic features, such as livingness, initiation efficiency, propagation rate, syndiospecificity and copolymerization ability. The synthesis of novel olefin block copolymers and their catalytic synthesis are also introduced using this living system.
Polymer Journal (2011) **43,** 331–351; doi:10.1038/pj.2011.13

Keywords: cycloolefin copolymer; living polymerization; norbornene; propene; single-site catalyst; syndiospecific polymerization; 1-alkene

A living polymerization system, in which neither chain transfer nor deactivation occurs, affords polymers with predictable molecular weights and narrow molecular weight distributions (MWDs). Living polymerization techniques are utilized for the synthesis of terminally functionalized polymers and block copolymers. Another feature of living polymerization is its simple kinetics. Because neither chain transfer nor deactivation occurs in living polymerization, the number of polymer chains (N) is equal to the number of active centers ([C*]), and the number-average molecular weight (M_n) directly reflects the propagation rate. In living polymerization, the propagation rate can be evaluated from the M_n value and the polymerization time. As chain transfer via β-elimination and/or transmetalation with trialkylaluminum as a cocatalyst is inevitable in conventional Ziegler–Natta catalytic systems; homogeneous $V(acac)_3/Et_2AlCl$ (where acac is acetylacetonate or its analog) had previously been the only catalytic system that produced syndiotactic-rich living polypropylene (PP) at −78 °C.[1,2]

The development of metallocene catalysts has enabled us to produce a variety of uniform olefin copolymers and to control the stereoregularity of poly(1-alkene)s.[3,4] The success of metallocene catalysts has stimulated research on transition metal complexes for olefin polymerization,[5–7] so-called single-site catalysts, which has also resulted in various transition metal complexes for the living polymerization of olefins.[8,9]

We have also developed a living polymerization system using *ansa*-dimethysilylene(fluorenyl)(amido)dimethyltitanium, $Me_2Si(\eta^3\text{-}C_{13}H_8)(\eta^1\text{-}N^tBu)TiMe_2$ (**1**), combined with a suitable cocatalyst. The catalytic system allows not only a syndiospecific living polymerization of propene and a 1-alkene but also a living homopolymerization and copolymerization of norbornene with a 1-alkene. We investigated the effect of cocatalyst, solvent and the ligand of the titanium complex on propene polymerization in terms of the livingness of the system. We also synthesized novel olefin block copolymers with the living system. This article reviews the characteristics of **1**-based catalysts for tailor-made polyolefins.

SYNTHESIS AND STRUCTURES OF TITANIUM COMPLEXES

Synthesis of titanium complexes

The titanium complexes that appear in this article are shown in Scheme 1. The *ansa*-monocyclopentadienylamido ligand for olefin polymerization catalyst was originally introduced by Bercaw and colleagues[10] in a scandium complex, and the titanium complex with *ansa*-monocyclopentadienylamido ligand was first reported by Okuda[11] The commercial application of group IV *ansa*-monocyclopentadienylamido complexes was developed by Dow and Exxon and was named constrained geometry catalysts (CGCs) after the structure of the complexes. CGCs are superior in the copolymerization of ethene with 1-alkene or styrene compared with bis(cyclopentadienyl) group IV metal complexes and have been applied for the production of ethene-based copolymers such as linear low-density polyethylene. *Ansa*-$Me_2Si(\eta^5\text{-}C_5Me_4)(\eta^1\text{-}N^tBu)TiMe_2$ (**CGC-Ti** in Scheme 1) is a representative CGC.[12]

We succeeded in the synthesis of the fluorenyl derivative **1** of **CGC-Ti**, the synthetic routes of which are illustrated in Scheme 2. We originally synthesized **1** via route II from $TiCl_3$ and the ligand via multisteps with very low yields.[13] We applied route I,[14] which starts

Graduate School of Engineering, Hiroshima University, Hiroshima, Japan
Correspondence: Professor T Shiono, Graduate School of Engineering, Hiroshima University, Kagamiyama 1-4-1, Higashi-Hiroshima, Hiroshima 739-8527, Japan.
E-mail: tshiono@hiroshima-u.ac.jp
Received 19 December 2010; revised and accepted 20 January

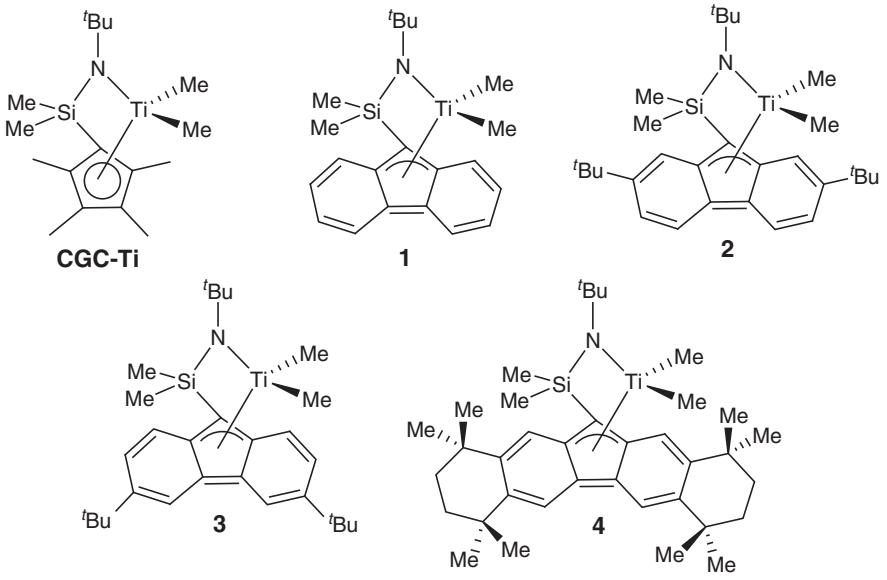

Scheme 1 Alkyltitanium complexes used in this study.

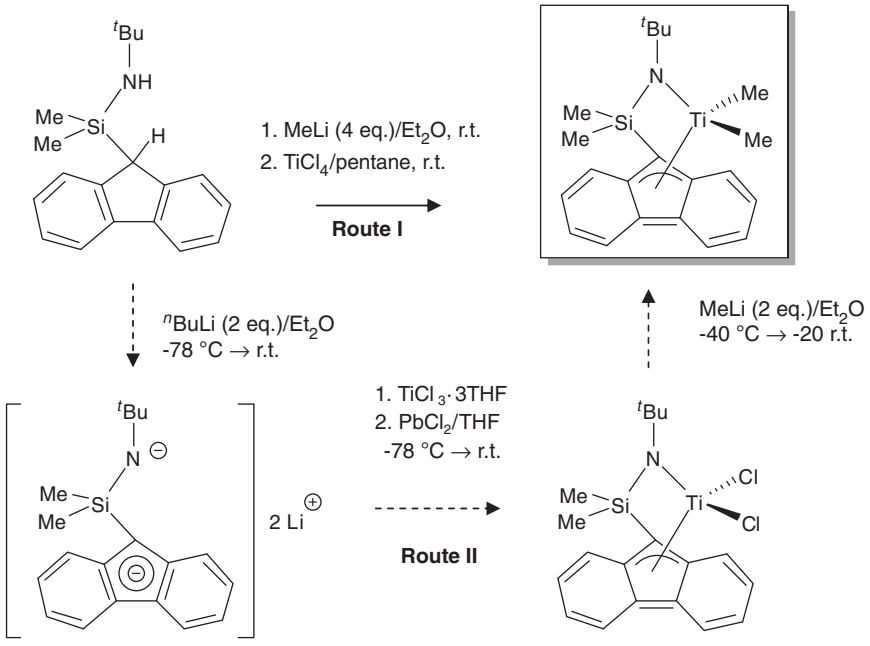

Scheme 2 Synthetic routes of **1**.

from $TiCl_4$, the ligand and four molar equivalent of MeLi, to give **1** through a one-pot synthesis and succeeded in the synthesis of **1** and Zr and Hf analogs (**1-Zr** and **1-Hf**) with 42–43% yields.[15] The fluorenyl derivatives **2–4**,[16,17] the indenyl derivative[18] and **CGC-Ti** were also synthesized by this procedure with 20–60% yields. All of these complexes were isolated as crystals, and their molecular structures were determined by single-crystal X-ray analyses.

The ORTEP drawings of **CGC-Ti** and **1** are illustrated in Figure 1. These complexes are activated via the abstraction of one of the two Me groups as Me^- to form coordinatively unsaturated cationic Ti–Me species, as shown in Equation (1). The polymerization begins by the coordination of monomer followed by the migratory insertion into the Ti–Me bond, and the propagation proceeds via successive monomer coordination and insertions.

$$L_2TiMe_2+LA \rightarrow [L_2TiMe]^+ + [Me\,LA]^- \quad (LA: \text{Lewis Acid}) \qquad (1)$$

The bond lengths from Ti to the cyclopentadienyl or the fluorenyl ligand determined by X-ray crystallography are summarized in Table 1. In **CGC-Ti**, the bond lengths between Ti and five carbons of the C_5Me_4 group are in the range 2.28–2.46 Å, indicating the η^5-coordination of the C_5Me_4 ligand. In contrast, the bond lengths between Ti and the fluorenyl ligand in **1** become elongated as follows: Ti-C^1 (2.25 Å) < Ti-C^2 (2.42 Å) < Ti-C^3 (2.57 Å). The other Ti fluorenyl derivatives, **2–4,** show the same tendency, indicating the

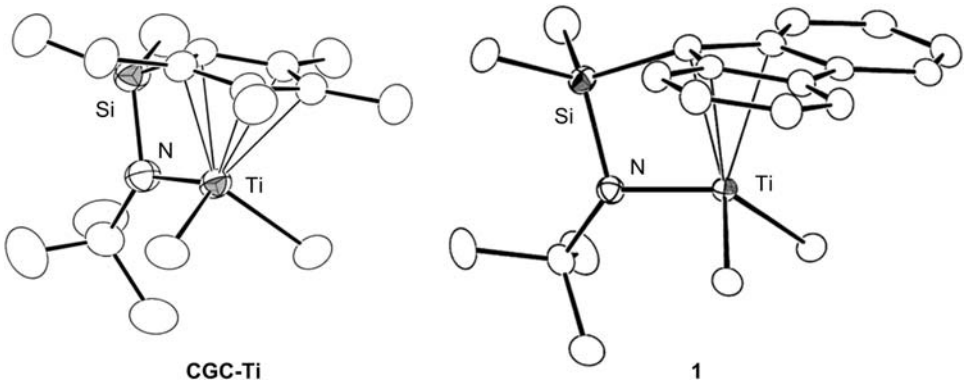

Figure 1 ORTEP diagrams of **CGC-Ti** and **1**.

Table 1 Bond lengths between metal and cyclopentadienyl ligand in CGC-Ti and 1–4

	Length (Å)						
Bond	***1***	***2***	***3***	***4***	*CGC-Ti*	*1-Zr*	*1-Hf*
Mt–C^1	2.252(3)	2.236(2)	2.247(3)	2.229(4)	2.283(3)	2.403(3)	2.401(5)
Mt–C^2	2.415(3)	2.470(2)	2.422(3)	2.424(4)	2.350(3)	2.529(2)	2.515(3)
Mt–C^3	2.572(3)	2.663(2)	2.619(3)	2.620(1)	2.463(3)	2.672(2)	2.664(3)
Mt–C^4	2.573(3)	2.620(2)	2.609(3)	2.589(1)	2.463(3)	2.672(2)	2.664(3)
Mt–C^5	2.418(3)	2.366(3)	2.401(3)	2.412(3)	2.350(3)	2.529(2)	2.515(3)
Mt–N	1.923(3)	1.917(3)	1.923(3)	1.902(4)	1.947(4)	2.063(2)	2.046(4)

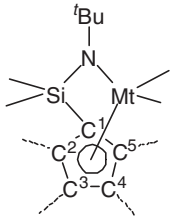

η^3-coordination of the fluorenyl ligand in the Ti complexes. In addition, the planar fused benz-groups of **1–4** are less bulky than the Me groups of **CGC-Ti**. These structural characteristics produce the open coordination site in the *ansa*-dimethylsilylene(fluorenyl)(amido)dimethyltitanium complexes, **1–4**, as compared with **CGC-Ti**. The difference in the bond length between Mt–C^1 and Mt–C^3 in **1** is 0.32 Å, whereas that between Mt–C^1 and the Zr and Hf analogs **1-Zr** and **1-Hf** is 0.27 Å and 0.26 Å, respectively, indicating that the tendency for η^3-coordination of the fluorenyl ligand is weakened in **1-Zr** and **1-Hf**.

POLYMERIZATION OF PROPENE AND HIGHER 1-ALKENE

Effects of cocatalyst

Propene polymerization was conducted by activating **1** with methylaluminoxane (MAO), $Ph_3CB(C_6F_5)_4$ or $B(C_6F_5)_3$ in toluene at 40, 0 and −50 °C by in-batch polymerization, where a certain amount of monomer was first charged. The results are shown in Table 2. In the case of $Ph_3CB(C_6F_5)_4$ and $B(C_6F_5)_3$, trioctylaluminum (Oct_3Al) was added as a scavenger. MAO showed the highest yields at 40 and 0 °C to give low molecular weight polymers with M_w/M_n values of 2.5 and 1.8, respectively. The *N* value was determined from the M_n value and the polymer yield. The ratios of *N* to the Ti complex used (*N*/Ti) were 85 and 38, respectively, indicating the occurrence

Table 2 Effects of activators on propene polymerization with 1[a]

Run	*Activator*	*Temp. (°C)*	*Yield (g)*	M_n [b] *(×10³)*	M_w/M_n [b]	*N/Ti*[c] *(mol/mol)*
1	MAO	40	3.0	1.8	2.5	85
2	MAO	0	3.0	4.0	1.8	38
3	MAO	−50	Trace	—	—	—
4	$Ph_3CB(C_5F_6)_4$	40	1.4	68.4	1.5	0.50
5	$Ph_3CB(C_5F_6)_4$	0	1.5	72.6	1.6	0.50
6	$Ph_3CB(C_5F_6)_4$	−50	0.2	28.7	2.1	0.15
7	$B(C_5F_6)_3$	40	1.6	45.1	1.5	0.93
8	$B(C_5F_6)_3$	0	2.5	52.1	1.6	1.18
9	$B(C_5F_6)_3$	−50	0.1	5.4	1.2	0.48

[a]Polymerization conditions: Runs 1–3, Ti=20 μmol, MAO(Al)=8000 μmol; Runs 4–9, Ti=40 μmol, B=40 μmol, Oct_3Al=800 μmol; toluene=30 ml, C_3H_6=3.5 g.
[b]Determined by GPC using PS standards by universal calibration.
[c]Number of polymer chains calculated from yield and M_n per Ti used.

of chain transfer reaction. In the ^{13}C nuclear magnetic resonance (NMR) data of the produced polymers, the resonances of terminal isopropyl group were observed in addition to the resonance of regioregular main-chain propene sequence. Any other resonance was not detected. The results clarified that the propene polymerization with this system proceeded via 1, 2-addition highly regiospecifically, and the chain transfer with Me_3Al in MAO selectively occurred as shown in Scheme 3.[13]

When $Ph_3CB(C_6F_5)_4$ or $B(C_6F_5)_3$ was used, propene polymerization proceeded although the yield was very low. The *N*/Ti values were close to or <1 irrespective of the polymerization temperature, indicating the suppression of chain transfer reactions compared with MAO. The polymers obtained with $B(C_6F_5)_3$ at −50 °C showed an M_w/M_n value of 1.2, which suggests the living polymerization with **1**–$B(C_6F_5)_3$. The time course of the polymerizations with $B(C_6F_5)_3$ and $Ph_3CB(C_6F_5)_4$ at −50 °C is shown in Figure 2.

The conversion increased almost linearly with increasing polymerization time when $B(C_6F_5)_3$ was used, whereas it saturated below 10% when $Ph_3CB(C_6F_5)_4$ was used (Figure 2a). The time dependences of the M_n values were similar to that of the conversions, namely the M_n value in the $B(C_6F_5)_3$ system was proportional to polymerization time, whereas that in the $Ph_3CB(C_6F_5)_4$ system showed a saturating tendency as shown in Figure 2b. These results indicate that the living polymerization of propene proceeded with **1**–$B(C_6F_5)_3$, whereas deactivation occurred in **1**–$Ph_3CB(C_6F_5)_4$ at −50 °C.[19]

The *N*/Ti value was almost constant during the polymerization, irrespective of the cocatalyst employed (Figure 2c). The *N*/Ti values

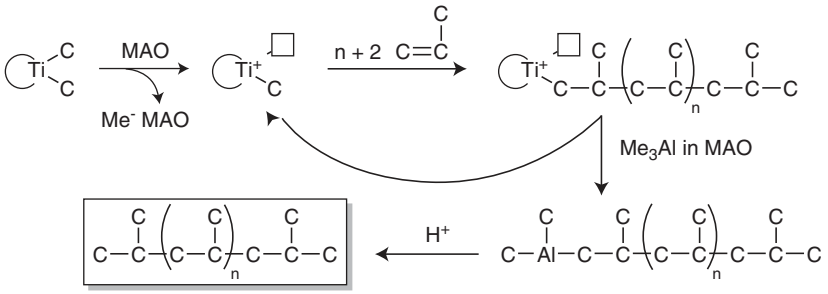

Scheme 3 Propene polymerization with **1**-MAO.

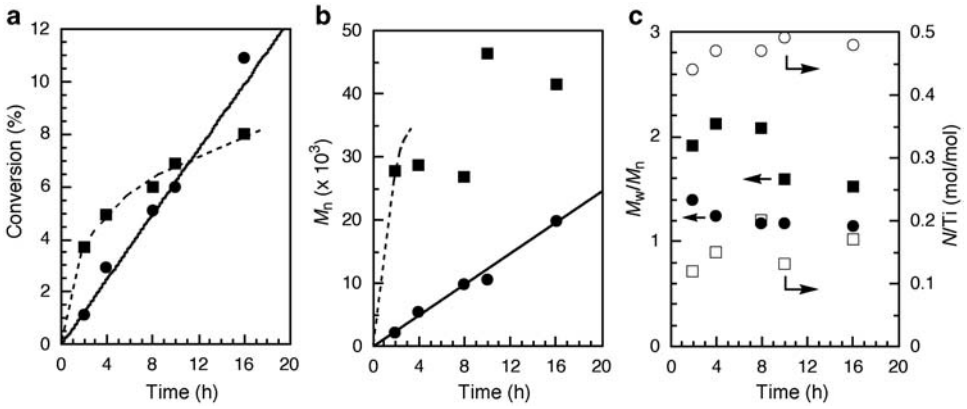

Figure 2 Kinetic profiles of propene polymerization with **1** activated with $B(C_6F_5)_3$ (●, ○) and $Ph_3CB(C_6F_5)_4$ (■, □). Polymerization conditions: Ti=B=40 μmol, Oct_3Al=800 μmol, toluene=30 ml, propene=3.5 g, temperature=−50 °C: time dependence of (**a**) conversion, (**b**) M_n, (**c**) M_w/M_n and *N*/Ti.[19]

Table 3 Effects of $B(C_6F_5)_3$ and Oct_3Al on propene polymerization with 1[a]

Run	*B/Ti (mol/mol)*	*Al/Ti (mol/mol)*	*Time (h)*	*Yield (g)*	*Conv. (%)*	M_n[b]	M_w/M_n[b] *(×10⁴)*	*N/Ti*[c] *(mol/mol)*[c]
10	1.0	20	12	0.32	9.1	1.5	1.2	0.55
11	1.3	20	12	1.44	41	5.2	1.1	0.70
12	1.5	20	12	2.27	65	7.6	1.1	0.75
13	2.0	20	12	2.75	79	8.6	1.1	0.80
14	2.0	0	0.5	trace	—	—	—	—
15	2.0	0	12	0.04	1.1	0.51	1.4	0.39
16	2.0	10	0.5	1.04	30	10.2	1.3	0.51

[a]Polymerization conditions: Runs 10–13, Ti=40 μmol, toluene=30 ml; Runs 14–16, Ti=20 μmol, toluene=10 ml; C_3H_6=3.5 g, temperature=−50 °C.
[b]Determined by GPC using PS standards by universal calibration.
[c]Number of polymer chains calculated from yield and M_n.

indicate that about a half of the total Ti was active during the polymerization in **1**–$B(C_6F_5)_3$, whereas only about 15% of Ti was converted into active species in **1**–$Ph_3CB(C_6F_5)_4$.

Because the *N*/Ti values were constant during the polymerization, the slope of M_n versus polymerization time plots in Figure 2b corresponds to the propagation rate constant of each system. The initial slopes indicate that the Ti species activated with $Ph_3CB(C_6F_5)_4$ was more than 10 times as active as that activated with $B(C_6F_5)_3$, although it was quickly deactivated.

These phenomena are interpreted as an interaction between the cationic Ti active species and the counter anion.[20] $B(C_6F_5)_3$ partly abstracts the alkyl ligand to form 'cation-like' active species as shown in Equation (2), whereas $Ph_3CB(C_6F_5)_4$ gives the non-coordinating counter anion of $[B(C_6F_5)_4]^-$ according to Equation (3). The former is less active but more stable in producing a living polymer.

$$L_2TiMe_2+B(C_6F_5)_3 \rightleftarrows [L_2TiMe^+\text{---}Me\text{-}B(C_6F_5)_3^-] \quad (2)$$

$$L_2TiMe_2+Ph_3CB(C_6F_5)_4 \rightarrow [L_2TiMe]^+[B(C_6F_5)_4]^-+Ph_3CMe \quad (3)$$

Because the activation process with $B(C_6F_5)_3$ in Equation (2) is an equilibrium reaction, excess $B(C_6F_5)_3$ should be favored to increase the initiation efficiency. The effects of additional $B(C_6F_5)_3$ were clearly observed, as shown in Table 3 (Runs 10–13). A small excess of $B(C_6F_5)_3$ improved the conversion by a factor of 4.5, accompanied by the increase in the M_n value by a factor of 3.5; however, the *N*/Ti value increased by only a factor of ~1.3. The further addition of $B(C_6F_5)_3$ increased the M_n value much more than the *N*/Ti value.

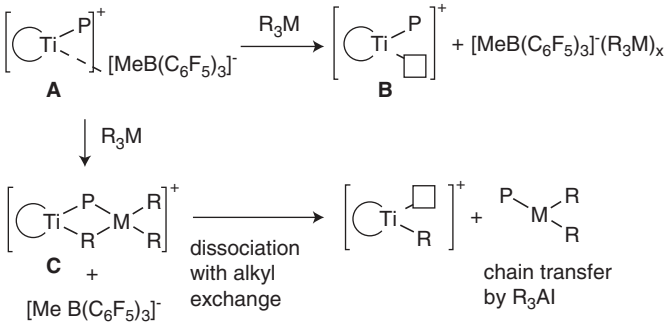

Scheme 4 Plausible reactions of $B(C_6F_5)_3$ and trialkylaluminum with the active Ti species.

Table 4 Additive effects of trialkylaluminum on propene polymerization with 1-$B(C_6F_5)_3$ at −50 °C[a]

Run	*Additive (g)*	*Yield (%)*	*Conv. (×10⁻⁴)*	M_n	M_w/M_n *(mol/mol)*	*N[b]/Ti*
17	Me_3Al	Trace	—	—	—	—
18	Et_3Al	0.65	72	0.46	1.6	7.2
19	$^iBu_3Al$	0.03	3.3	0.41	1.2	0.38
20	Oct_3Al	0.78	87	6.1	1.3	0.64

[a]Polymerization conditions: Ti=$B(C_6F_5)_3$=20 μmol, toluene=10 ml, [Al]/[Ti]=100, C_3H_6=0.9 g, time=30 min.
[b]Number of polymer chains.

It should be noted that the polymerization was conducted in a batch-type operation in which the increase of the M_n value is underestimated. These results imply that the main effect of excess $B(C_6F_5)_3$ is to enhance the propagation rate.[21]

Oct_3Al, which had previously been regarded as a scavenger, was also found to enhance the propagation rate. The polymer was obtained even in the absence of Oct_3Al, although the propagation rate was very low (Runs 14 and 15): the M_n value of the polymer reached 5100 after 12-h polymerization. The addition of Oct_3Al (Al/Ti=10) greatly promotes the propagation rate to give the polymer with an M_n value of 102 000 in 30 min (Run 16).

The enhancement of propagation rate by the addition of $B(C_6F_5)_3$ and Oct_3Al can be interpreted by observing Scheme 4. An electron-deficient group 13 compound (R_3M, where M is B or Al) can interact with the ion pair of the active species (**A**) in two ways. One is the coordination with the counter anion to give the coordinatively unsaturated Ti cationic species (**B**), and the other is the formation of hetero-bimetallic species with the cationic Ti species (**C**). If coordination to the counter anion selectively occurs, which should be the case of $B(C_6F_5)_3$ and Oct_3Al, the activity is increased by the formation of highly active coordinatively unsaturated Ti species **B**.

When the hetero-bimetallic species **C** is formed, two possibilities can be considered. If the coordination of R_3M to the Ti species is in equilibrium, the chain transfer to R_3M should occur. If **C** is very stable, the activity should be suppressed. The formation and the stability of **C** should depend on R in R_3M as well as on the ligand of the Ti complex. The effects of various R_3Al were, therefore, investigated in the propene polymerization with **1**–$B(C_6F_5)_3$ at −50 °C (Table 4).[22] The polymerization features strongly depended on the added R in R_3Al. The polymer yield decreased in the following order: $Oct_3Al \geqslant Et_3Al \gg {}^iBu_3Al > Me_3Al=0$. Although Et_3Al and Oct_3Al afforded polymers in similar yields, the M_n value with Et_3Al was one order of magnitude lower than that with Oct_3Al to give the *N*/Ti value of 7.2. The result shows the high chain transfer ability of Et_3Al, indicating that the coordination of Et_3Al to the cationic Ti species is in equilibrium under the present conditions. The M_n value with $^iBu_3Al$ was also one order of magnitude lower than that with Oct_3Al, but the *N*/Ti value was almost the same as that with Oct_3Al. In addition, the M_w/M_n value with $^iBu_3Al$ was 1.3. These results indicate that the living polymerization also proceeded in the presence of $^iBu_3Al$ although the rate enhancement by $^iBu_3Al$ was one order of magnitude lower than that by Oct_3Al. The very poor polymer yield with Me_3Al can be interpreted by the formation of the stable hetero-binuclear species.

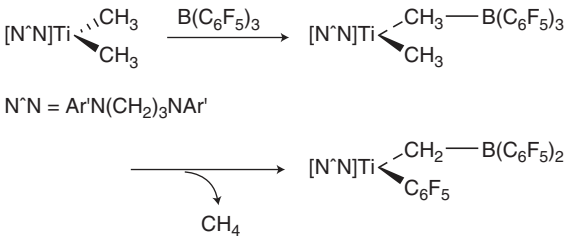

Scheme 5 Deactivation of $[Ar'N(CH_2)_3NAr']TiMe_2$–$B(C_6F_5)_3$.

As described above, it was proved that the living polymerization of propene proceeded with **1** activated by $B(C_6F_5)_3$ at −50 °C in toluene, and the propagation rate was enhanced by the addition of excess $B(C_6F_5)_3$ and/or a suitable amount of Oct_3Al.

Activation with Me_3Al-free MAO

McConville and Scollard[23] demonstrated the living polymerization of higher 1-alkene at 23 °C with $[Ar'N(CH_2)_3NAr']TiMe_2$ (Ar'=2,6-$^iPrC_6H_3$ and so on) activated by an equimolar amount of $B(C_6F_5)_3$. They clarified, however, that the catalytic system was deactivated in the absence of monomer accompanied by evolving methane, according to Scheme 5.[24] They also reported that the use of MAO in place of $B(C_6F_5)_3$ produced more thermally stable active species, although chain transfer to Me_3Al selectively occurred.[25]

In the propene polymerization with **1**, MAO showed higher activity than with $B(C_6F_5)_3$ at 0 °C and 40 °C to give low molecular weight PP via selective chain transfer to Me_3Al shown in Scheme 3. If the deactivation of the **1**–$B(C_6F_5)_3$ system at elevated temperature occurs via the reaction between the cationic Ti species and $[MeB(C_6F_5)_3]$ similar to the $[Ar'N(CH_2)_3NAr']TiMe_2$–$B(C_6F_5)_3$ system, the deactivation process can be eliminated by the use of MAO in place of $B(C_6F_5)_3$. In addition, if Me_3Al is absent in MAO, the chain transfer reaction can also be eliminated to produce a living polymerization system. We therefore prepared Me_3Al-free MAO by vacuum drying a toluene solution of MAO, followed by washing with hexane and applying it as a cocatalyst.[26] Thereafter, the MAO treated via this procedure was denoted as dMAO, an abbreviation of dried MAO. Figure 3 shows the ^1H NMR spectra of MAO and dMAO, which indicates that dMAO does not contain free Me_3Al.

Propene polymerization was conducted with **1** at 0 °C using MAO or dMAO as a cocatalyst in a semi-batch system, in which the propene pressure was kept at atmospheric pressure during the polymerization, and the consumed monomer was continuously supplied.[26] Hence, the polymerization rate can be monitored by the flow rate of propene introduced. **CGC-Ti** was also used for comparison.[27] The results are shown in Table 5. The polymerization time was changed in each experiment according to the catalytic activity because the produced polymer interfered with effective stirring.

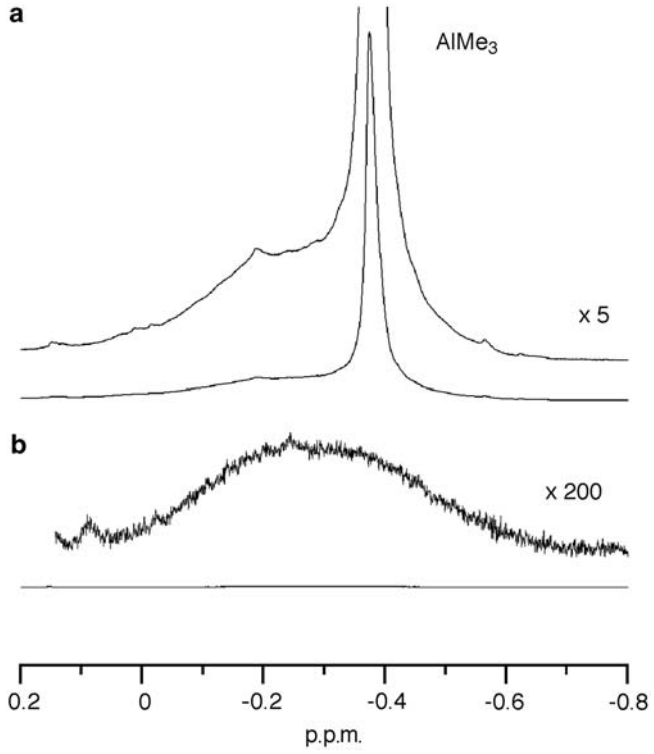

Figure 3 ^{1}H NMR spectra of MAO (**a**) and dMAO (**b**) in benzene-d_6.[26]

Table 5 Effects of activator on propene polymerization with 1 and CGC-Ti at 0 °C[a]

Run	*Catalyst*	*Cocatalyst*	*Time (min)*	*Yield (g)*	*Activity*[b]	M_n[c] ($\times 10^3$)	M_w/M_n[c]	*N/Ti*[d]
21	**1**	MAO	60	0.63	31	2.4	1.4	13
22	**1**	dMAO	30	2.57	257	157	1.2	0.82
23	**CGC-Ti**	MAO	90	0.47	16	13	2.2	1.81
24	**CGC-Ti**	dMAO	30	2.22	222	157	1.3	0.71

[a]Polymerization conditions: Ti=20 μmol, toluene=30 ml, MAO=8 mmol, propene=1 atm, temperature=0 °C.
[b]Activity=kg-PP mol-Ti^{-1} h^{-1}.
[c]Determined by GPC.
[d]Calculated from yield and M_n.

The activities with dMAO were one order of magnitude higher than that with MAO irrespective of the titanium complexes employed. The M_n values were also one or two orders of magnitude larger in the dMAO systems than the MAO systems. The polymers obtained with the dMAO systems showed an M_w/M_n value of ~1.2, suggesting the living nature of propene polymerization with **1** and **CGC-Ti** using dMAO as a cocatalyst.

To investigate the livingness of the **1**–dMAO and **CGC-Ti**–dMAO systems, propene polymerization was conducted at 0 °C in toluene with batch operation by changing the amount of monomer fed. Regardless of the titanium complex, polymerization proceeded quantitatively within 1 h. Figure 4 displays the relation between the yield and the M_n value. The M_n value increased against the yield in both systems. The linearity was, however, better in the **1**–dMAO system than in the **CGC-Ti**–dMAO system. In the **1**–dMAO system, the *N*/Ti value was almost constant, whereas it gradually increased in the **CGC-Ti**–dMAO system, accompanied by an increase in the M_w/M_n value. The results indicate that the chain transfer reaction occurred in the latter system under these conditions. The post-polymerization also

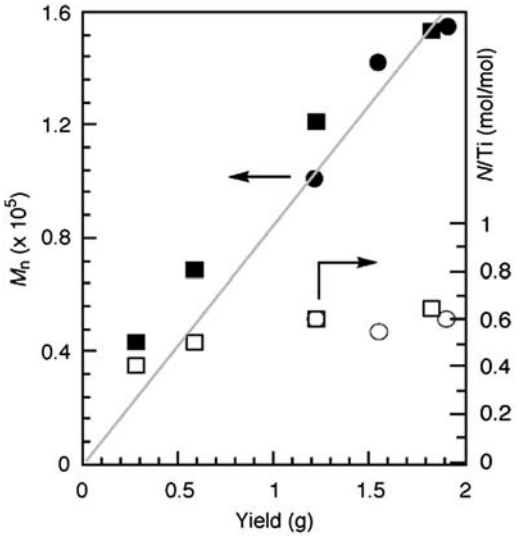

Figure 4 Plots of M_n and *N*/Ti against yield in propene polymerization with dMAO: ■, □; **CGC-Ti**: ●, ○, **1**. Polymerization conditions: 1 h; for other conditions, see Table 5.

supports the formation of living PP with **1**–dMAO at 0 °C. The use of dMAO in place of $B(C_6F_5)_3$ was found to raise the living polymerization temperature of **1** to 0 °C.

The lower activity and lower molecular weight observed with MAO can be ascribed to the presence of Me_3Al, which forms heterobinuclear species **C** in Scheme 4. The M_n and *N*/Ti values with MAO and dMAO in Table 5 indicate that chain transfer with Me_3Al frequently occurred in the **1**–MAO system but rarely in the **CGC-Ti**–MAO system.

Activation with R_3Al-free modified MAO (MMAO)

As the active species in Ti complexes for olefin polymerization is an ion pair, as shown in Equation (1), the activity, namely [C*] and the propagation rate constant (k_p) should depend on the solvent employed. In living polymerization, the [C*] value is equal to the *N* value determined from the polymer yield and the M_n value; the k_p value can be directly evaluated from the M_n value and the polymerization time.

McConville and Scollard investigated the effects of solvents in the living polymerization of 1-alkene with $[Ar'N(CH_2)_3NAr']TiMe_2$–$B(C_6F_5)_3$ by replacing a part of the 1-alkene with CH_2Cl_2 or toluene.[23] The replacement with CH_2Cl_2 increased the M_n value by a factor of ~30, which can be attributed to the charge separation of the ion pair by the polarity of CH_2Cl_2, although the initiation efficiency was reduced. The replacement with toluene suppresses the activity because of the formation of the Ti η^6-toluene species.

We succeeded in the living polymerization of propene with **1**–dMAO in toluene at 0 °C, the kinetics of which should also depend on the solvent employed. However, the solubility of MAO in saturated hydrocarbons such as hexane is not good and further decreases after the removal of Me_3Al to obtain dMAO. MMAO, which is the condensation product of water and the mixture of Me_3Al and $^iBu_3Al$, possesses higher solubility than MAO and is easily soluble in hexane. We therefore removed the remaining Me_3Al and $^iBu_3Al$ in MMAO by repeated vacuum drying and successive redissolving in heptanes to obtain R_3Al-free MMAO (dMMAO).[28] Figure 5 shows the ^{1}H NMR spectra of MMAO and dMMAO in tetrahydrofuran-d_8. The contents of each Al species were calculated from the relative intensities

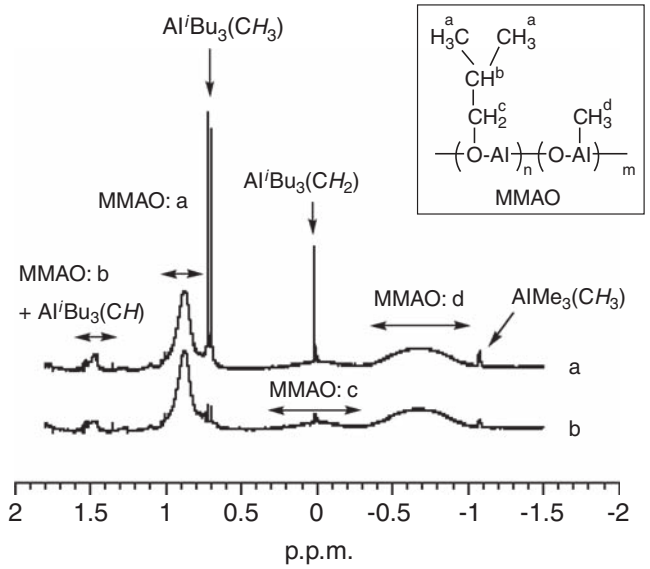

Figure 5 ^{1}H NMR spectra of MMAO (**a**) and dMMAO (**b**) in THF-d_8.[29]

Table 6 Composition of MMAO and dMMAO

Al species	*Me_3Al (mol%-Al)*	*$^iBu_3Al$*	*MMAO*
MMAO	0.1	1.3	98.6
dMMAO	0.1	0.1	99.8

Table 7 Effect of activator on propene polymerization with 1 in heptane[a]

Run	*Cocatalyst*	*Conv. (%)*	M_n[b] *($\times 10^4$)*	M_w/M_n[b]
25	dMAO	65	4.26	2.10
26	dMMAO	100	9.93	1.32

[a]Polymerization conditions: heptane =30 ml, Ti=20 μmol, Al=8.0 mmol, propene=1.26 g, temperature=0 °C, 1 h.
[b]Determined by GPC using universal calibration.

in the ^{1}H NMR spectra, as shown in Table 6, which indicates that the treatment reduced the contents of Me_3Al and $^iBu_3Al$ to ~0.2 mol% of the total Al species.[29]

Propene polymerization by a batch method was then conducted with **1** activated by dMAO or dMMAO in heptane (Table 7).[30] The dMAO system produced the polymer at a 65% conversion with a broad MWD (M_w/M_n=2.10) for 1-h polymerization, whereas the dMMAO system quantitatively produced the polymer with a narrow MWD (M_w/M_n=1.32). The broad MWD using dMAO in heptane is mainly attributed to the low solubility of dMAO: dMMAO is perfectly soluble in heptane, whereas dMAO is sparingly soluble in heptane under the polymerization conditions. The heterogeneity of the precipitated dMAO should have caused the broadening of MWD. We also succeeded in the living polymerization of propene with the [Ar'N(CH$_2$)$_3$NAr']TiMe$_2$–dMMAO (Ar'=2,6-^{i}Pr$_2$C$_6$H$_3$) system in heptane at 0 °C.[28]

As the potential of dMMAO as a cocatalyst in heptane was confirmed, we investigated the effect of solvents, namely toluene, chlorobenzene (CB) and *ortho*-dichlorobenzene (*o*-DCB), on propene polymerization with **1**–dMMAO by a batch method conducted over 1 h.[30] The polymerizations quantitatively proceeded, irrespective of the amount of propene charged and the solvent employed. The

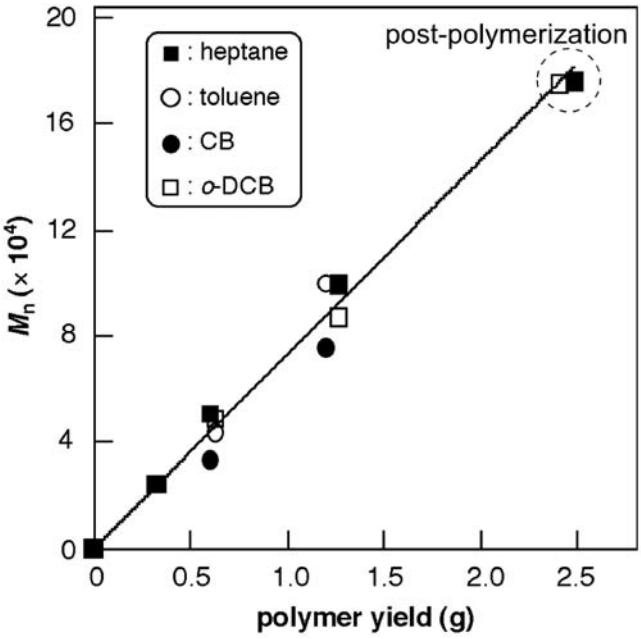

Figure 6 Plots of M_n versus polymer yield in propene polymerization with **1**–dMMAO at 0 °C in heptane, toluene, CB and *o*-DCB. Polymerization conditions: Ti=20 μmol, dMMAO=8.0 mmol, solvent=30 ml, propene=1.26 g, temperature=0 °C, 1 h. Post-polymerization conditions: propene=1.26 g, 1 h.[30]

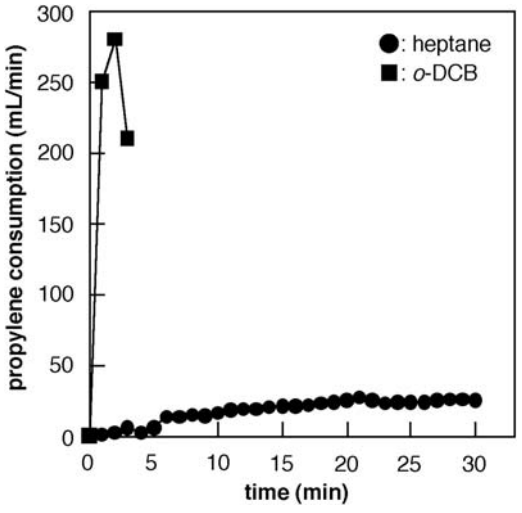

Figure 7 Rate-time profiles of propene polymerization with **1**–dMMAO at 0 °C in heptane and *o*-DCB. Polymerization conditions: Ti=20 μmol, norbornene=1.2 M, total volume (toluene + norbornene)=30 ml, temperature=20 °C, 3 min.[30]

produced polymers showed narrow MWDs of 1.14~1.39. The M_n values are plotted against the polymer yields in Figure 6, which form a straight line through the origin regardless of the solvent employed.

To confirm the livingness of the systems, we conducted post-polymerization in heptane and *o*-DCB, which have the lowest and the highest dielectric constant, respectively, among the solvents employed. The values are located on the same straight line, as shown in Figure 6. These results indicate that the living polymerization of propene proceeded in all of the solvents with **1**–dMMAO, and the initiation efficiency was independent of the solvent employed.

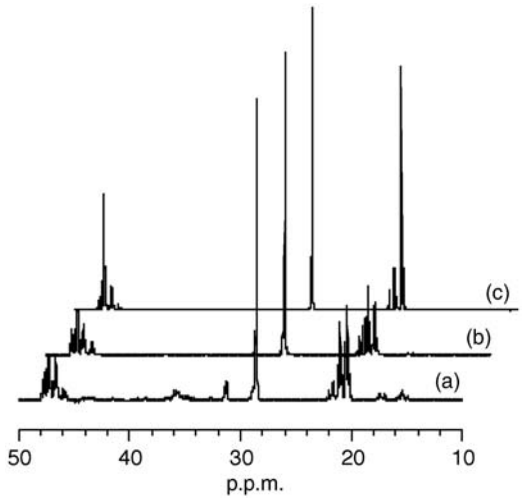

Figure 8 ^{13}C NMR spectra of PPs obtained with dMAO as a cocatalyst: (**a**) $(\eta^5\text{-}C_5Me_5)Ti(CH_2Ph)_3$; (**b**) **CGC-Ti** and (**c**) **1**.

Table 8 Microstructures of PPs obtained with cyclopentadienylalkyltitanium–dMAO systems

Run	*Catalyst*	*[mm]*[a]	*[mr]*[a]	*[rr]*[a]	*CI*[b]
22	**1**	0.06	0.27	0.67	ND
24	**CGC-Ti**	0.14	0.49	0.37	0.01
—	$(\eta^5\text{-}C_5Me_5)Ti(CH_2Ph)_3$	0.15	0.48	0.37	0.13

Abbreviation: ND, not determined.
[a]Determined by 125 MHz ^{13}C NMR.
[b]Determined from the resonances of the methine carbons by the following equation: chemical inversion=$[T_{\beta\gamma}]/([T_{\beta\beta}]+[T_{\beta\gamma}]+[T_{\alpha\beta}]+[T_{\alpha\gamma}])$.

The effects of the solvents on the kinetic features were then investigated using a semi-batch method. Propene polymerization was conducted in heptane and *o*-DCB under atmospheric pressure; the other conditions were the same as those of the batch method, except that 5 μmol of **1** was employed. The kinetic profiles thus obtained are shown in Figure 7.

Even when 5 μmol of Ti was employed, the *o*-DCB system showed very high activity, and stirring was stopped within 3 min. In contrast, the consumption rate of propene in the heptane system gradually increased and reached a steady value.

Because the initiation efficiency was the same in heptanes as it was in *o*-DCB, as shown in Figure 6, the high activity in *o*-DCB can be ascribed to a high propagation rate. The reason why the propagation rate increased can be explained by the enhancement in the separation of the active Ti cation and the dMMAO-derived anion in the polar solvent. Fink *et al.*[31] reported the linear relationship between the polarity of the solvent and the polymerization rate. Our results clearly indicate that the rate enhancement with the polar solvent is ascribed to the increase in the k_p value.

Structure of PP

The ^{13}C NMR spectra of the PPs obtained with **1**, **CGC-Ti** and $(\eta^5\text{-}C_5Me_5)Ti(CH_2Ph)_3$ activated by dMAO in toluene are illustrated in Figure 8. The contents of steric triad and chemical inversion were determined from the spectra, and the results are summarized in Table 8.

Both the regioregularities and stereoregularities of the PPs depended on the titanium complexes used. $(\eta^5\text{-}C_5Me_5)Ti(CH_2Ph)_3$ gave a slightly sydiotactic-rich polymer with more than 10% regioirregular units, whereas **CGC-Ti** produced an almost atactic polymer with about 1% of regioirregular units, as reported by Waymouth and colleagues.[32] In contrast, **1** was highly regiospecific and produced a syndiotactic-rich polymer, the syndiotacticity of which was almost the same as that of the polymers obtained with the V-based living polymerization catalyst at very low temperature.[1,33] Waymouth and colleagues[32] found that the corresponding Zr complex, *ansa*-Me_2Si

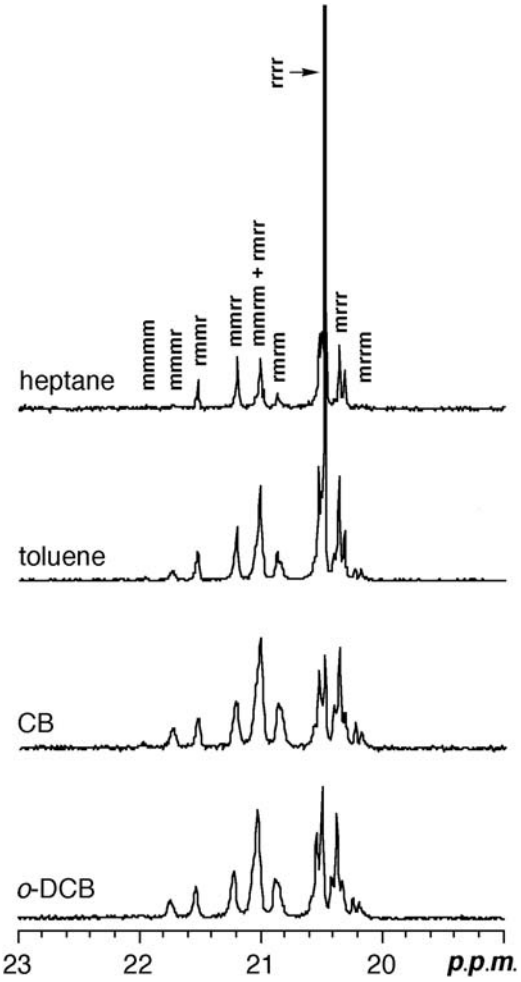

Figure 9 125 MHz ^{13}C NMR spectra of methyl regions of PPs obtained with **1**–dMMAO at 0 °C in heptane, toluene, CB and *o*-DCB.[30]

Table 9 Steric pentad distribution of PPs obtained with 1–dMMAO in various solvents

Pentad[a]	*Heptane*[b]	*Heptane*	*Toluene*	*CB*	*o-DCB*
mmmm	0.00	0.00	0.00	0.01	0.01
mmmr	0.01	0.00	0.02	0.04	0.04
rmmr	0.04	0.04	0.04	0.05	0.05
mmrr	0.08	0.09	0.08	0.10	0.10
mmrm+rmrr	0.10	0.10	0.19	0.26	0.24
rmrm	0.03	0.04	0.07	0.12	0.10
rrrr	0.60	0.60	0.39	0.19	0.23
mrrr	0.14	0.13	0.19	0.19	0.19
mrrm	0.00	0.00	0.02	0.04	0.04

[a]Determined by 125 MHz ^{13}C NMR.
[b]dMAO=8.0 mmol.

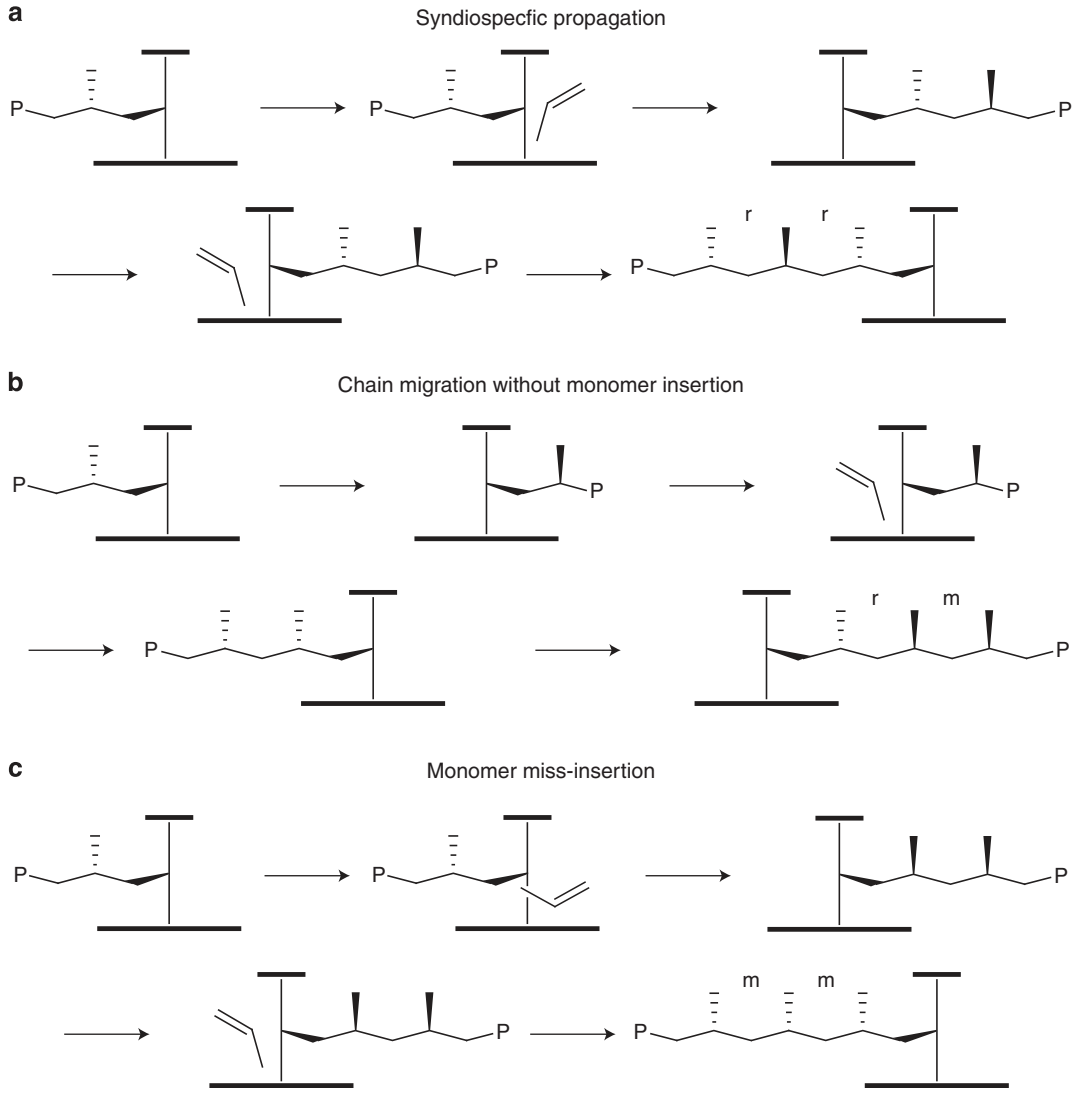

Scheme 6 Enantiomorphic site-controlled syndiospecific polymerization by C_s symmetric catalysts.

(η^5-$C_{13}H_8$)(η^1-^{t}BuN)$ZrCl_2$, combined with MAO yielded exceptionally regioregular PP and reported that the high regiospecificity could be ascribed to the Zr atom or the fluorenyl ligand because they could not isolate the corresponding Ti complex. The high regiospecificity of **1** implies that the fluorenyl ligand has an important role in the control of regiospecificity.

Living PPs were obtained in various solvents by **1**–dMMAO. The high regiospecificity of **1** was maintained in all the solvents used, but the stereospecificity was significantly affected by the solvent. The ^{13}C NMR spectra of the PPs in methyl regions are illustrated in Figure 9. The resonance of the syndiotactic pentad, rrrr, became stronger in the following order, CB = *o*-DCB < toluene < heptane.

The steric pentad distributions determined from the spectra are shown in Table 9, in which the data of the PP obtained by **1**–dMAO in toluene are also indicated for comparison. The pentad values indicate that the syndiotacticity of the PPs obtained with dMAO and dMMAO was almost the same but depended on the solvents used. Fink *et al.*[31] studied propene polymerization with *ansa*-$Me_2C(Flu)(Cp)ZrCl_2$–MAO in toluene/CH_2Cl_2 mixture and found that the rrrr pentads of the produced PPs monotonously decreased from 89% in pure toluene to 42% in pure CH_2Cl_2. They proposed that the decrease in the stereospecificity in the polar solvents may be caused by the isomerization of the solvent-separated zirconocene species via migration of the growing polymer chain without monomer insertion. Marks and Chen[34] also reported the effect of cocatalysts and solvents (toluene and *o*-DCB) on the kinetics and the stereospecificity of propene polymerization with *ansa*-$Me_2C(Flu)(Cp)ZrMe_2$. Busico *et al.*[35] reported a detailed kinetic model of propene polymerization with *ansa*-$R_2C(Flu)(Cp)ZrX_2$ (where R is Me and Ph, and X is Me and Cl) on the basis of the microstructure of the produced polymers and discussed the effect of cocatalysts and solvents (toluene and bromobenzene). These papers report that the decrease in syndiospecificity with the C_s-symmetry zirconocene catalysts in polar solvent is ascribed to the 'chain migration without monomer insertion (skipped insertion)' and not to the 'selection miss of enantioface' (Scheme 6).[36]

The change in the syndiospecificity observed by the present Ti complex can be also interpreted by the separation of an active ion pair. The dMMAO–polar solvent system produces a solvent-separated ion pair and, hence, allows the growing chain to migrate between the two enantiotopic sites on the Ti cation without monomer insertion. In contrast, the dMMAO–heptane system favors the contact ion pair and prohibits the migration of the growing chain.

Table 10 Propene polymerization with 1–4 activated by dMMAO in heptane

Run	Catalyst	Al/Ti[a] (mol/mol)	Time (min)	Activity[b]	M_n[c] ($\times 10^4$)	M_w/M_n[c]	N/Ti[d] (mol/mol)
27	**1**	400	11	660	16.1	1.31	0.75
28	**2**	400	3	2280	20.8	1.65	0.55
29	**3**	400	3	2320	19.6	1.46	0.60
30	**2**	200	9	787	20.2	1.68	0.60
31	**3**	200	7	916	16.9	1.45	0.65
32	**3**	100	17	326	15.2	1.48	0.60
33	**4**	100	0.5	11 400	19.3	2.92	0.50

Polymerization conditions: heptane=30 ml, Ti=20 μmol, cocatalyst=dMMAO, propene=1 atm at 0 °C.
[a]Al/Ti=molar ratio.
[b]Activity in kg-polymer mol-Ti^{-1} h^{-1}.
[c]Determined by GPC.
[d]The ratio of the number of polymer chains per Ti complex used.

Actually, the number of stereodefects (•••rmrr•••) arising from the 'chain migration' increased in the following order, as shown in Table 9: heptane (10%) < toluene (19%) < *o*-DCB (24%) < CB (26%). The number of stereodefects (•••rmmr•••) arising from the 'selection miss' is almost independent of the solvent employed (4∼5%). We can therefore conclude that the enhancement of syndiospecificity in heptane is ascribed to the suppression of the 'chain migration' and not to the selectivity of the prochiral face.

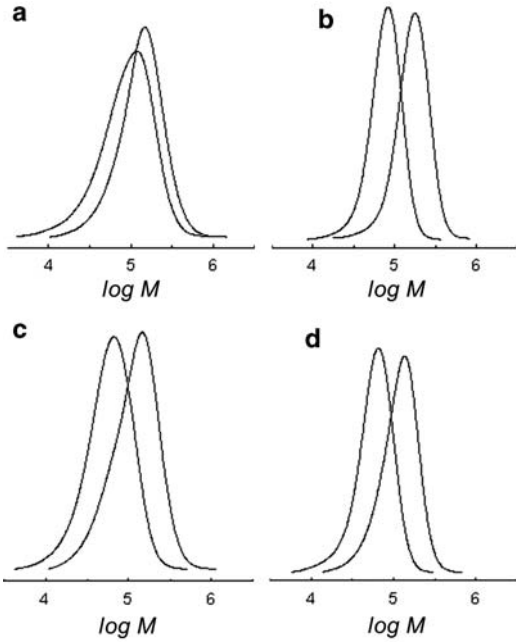

Figure 10 GPC curves of PPs obtained in post-polymerization: (**a**) **2**–dMMAO at 0 °C; (**b**) **2**–dMMAO at 25 °C; (**c**) **3**–dMMAO at 0 °C and (**d**) **3**–dMMAO at 25 °C.[16]

Substituent effects on the fluorenyl ligand

The use of dMMAO facilitated the living polymerization of propene in heptane, which afforded PP with the highest syndiotacticity among the solvents employed. We therefore investigated the propene polymerization with **2**, **3** and **4** in heptane activated by dMMAO.[16,17] The results of semi-batch polymerizations are summarized in Table 10; the polymerizations were terminated by the addition of acidic methanol before the polymer produced began to interfere with the stirring. When the polymerization was too fast to precisely evaluate the activity, the amount of dMMAO was also reduced.

The activities of 2,7-^{t}Bu$_2$-substituted **2** and 3,6-^{t}Bu$_2$-substituted **3** with Al/Ti=400 were 2280 and 2320 kg-PP·mol-Ti^{-1} h^{-1}, respectively, which were approximately three times higher than that of the non-substituted **1**. The activities were reduced to 787 kg-PP·mol-Ti^{-1} h^{-1} and 916 kg-PP·mol-Ti^{-1} h^{-1} with Al/Ti=200. These results indicate that the rate enhancement by the introduction of the ^{t}Bu groups is mainly ascribed to an electronic effect, although the 3,6-position is slightly superior to the 2,7-position. Complex **4**, which is the 2,3,6,7-^{t}Bu$_4$-substituted analog of **1**, showed the highest activity of 11 400 kg-PP·mol-Ti^{-1} h^{-1} among the four complexes, even with Al/Ti=100. The activity of **3** with Al/Ti=100 was 326 kg-PP·mol-Ti^{-1} h^{-1}.

The effects of the Al/Ti ratio on propene polymerization with **3**–dMMAO (Runs 29, 31 and 32) indicate that a large excess of dMMAO is necessary for a high propagation rate because the activity increased at a constant *N*/Ti value. Similar phenomena were also observed in propene polymerization with **1**–B(C$_6$F$_5$)$_3$, where excess B(C$_6$F$_5$)$_3$ or the addition of Oct$_3$Al enhanced the propagation rate.

The M_n values of the PPs obtained were as high as 15–20$\times 10^4$ with an M_w/M_n value of 1.5–1.7, except that obtained with **4**, and the *N*/Ti values were 0.50–0.65. Post-polymerization, in which the same amount of monomer was sequentially added after the first polymerization was completed, was then conducted with **2** and **3** at 0 °C and 25 °C. The gel permeation chromatography (GPC) curves of the produced PPs are illustrated in Figure 10, and the results are summarized in Table 11. The post-polymerizations proceeded quantitatively, and the GPC curves were shifted to higher molecular weight regions while maintaining the MWD narrow and the *N*/Ti value constant regardless of the Ti complex and the polymerization temperature. The results indicate the living nature of these systems. The MWDs of the batch polymerizations (Table 11) were narrower than that of the semi-batch polymerization (Table 10), which suggests that the broader MWD should be partly due to the physical inhomogeneity of the system caused by the heat of polymerization and/or ineffective stirring. The slow initiation in heptanes, as observed in Figure 7, should also broaden the MWD.

The MWD of the PP obtained with **4** after 30-s polymerization was very broad (M_w/M_n=2.9), although the *N*/Ti value was only 0.50. Batch polymerization of propene with **4** was conducted in heptane at 0 °C by changing the amount of propene charged. The polymerizations proceeded quantitatively to produce polymers with broad M_w/M_n values of ∼3. The M_n values of the produced polymers are plotted against the polymer yields in Figure 11, which shows a straight line through the origin. The results indicate that the chain transfer reactions did not occur during the polymerization, although the MWDs were broad. Post-polymerization was then conducted with **4**–dMMAO in heptane at 0 °C.

The GPC curves before and after the post-polymerization are illustrated in Figure 12 together with the results of the polymerizations. Although the polymerizations proceeded quantitatively during both stages, the M_n values did not double but only slightly increased and were accompanied by a narrow MWD. The peaks of the GPC curves remained almost unchanged, and the decrease in both the low and high molecular weight fractions produced a narrower MWD during the second stage. Considering the good linear relationship between the yield and M_n in Figure 11, we can conclude that chain transfer selectively occurred, probably due to the remaining ^{i}Bu$_3$Al in dMMAO after all of the monomers had been consumed. The narrower MWD during the second stage can be explained by the smooth

Table 11 Post-polymerization of propene with 2 and 3[a]

Run	*Catalyst*	*Propene (g)*	*Temp. (°C)*	*Time (min)*	*Yield (%)*	M_n[b] ($\times 10^4$)	M_w/M_n[b]	N[c] (*μmol*)
34	**2**	0.63	0	60	100	6.5	1.56	10
35	**2**	0.63+0.63	0	60+60	100	11.0	1.49	11
36	**2**	0.63	25	20	97	5.0	1.41	12
37	**2**	0.63+0.63	25	20+20	95	10.2	1.43	12
38	**3**	0.63	0	60	100	5.9	1.27	11
39	**3**	0.63+0.63	0	60+60	100	11.2	1.29	11
40	**3**	0.63	25	20	97	5.1	1.28	12
41	**3**	0.63+0.63	25	20+20	98	10.5	1.32	12

[a]Polymerization conditions: heptane=30 ml, Ti=20 μmol, Al=4.0 mmol.
[b]Number-average molecular weight and molecular weight distribution determined by GPC using universal calibration.
[c]Calculated from yield and M_n.

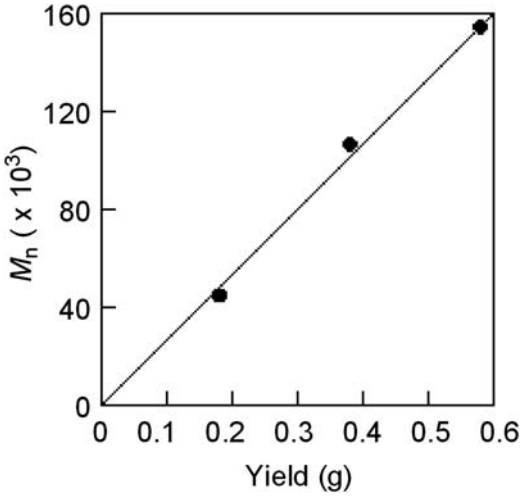

Figure 11 Plots of M_n against yield in propene polymerization with **4**–dMMAO in heptane.[17]

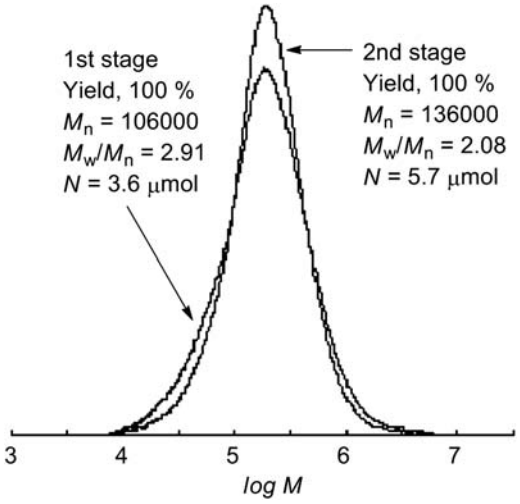

Figure 12 GPC curves of PPs before and after post-polymerization with **4**–dMMAO.[17]

initiation by the chain-transferred active species. The broad MWD by **4**, as compared with the other Ti complexes, can be partly ascribed to the high propagation rate of **4**, which makes the effect of slow initiation on the MWD more significant. In addition, the extremely high activity should induce physical inhomogeneity in the reactor, namely temperature and propene concentration, because of the insufficient removal of heat and stirring.

The substituent of the fluorenyl ligand also affected the stereospecificity of the Ti complexes. Table 12 summarizes the steric pentad distribution of the PPs obtained in heptane at 0 °C. The syndiotactic pentad (rrrr) of the PPs decreased in the following order: **3** (0.86) > **2** (0.69) > **1** (0.60) > **4** (0.45). Considering the similar geometry of **3** and **4** in the coordination site of propene, the syndiospecificity of **4** being the lowest is very strange.

Miller *et al.*[37–39] reported that the diethyl-ether-coordinated Zr analog of **4**, in which the fluorenyl ligand is coordinated to Zr in η^1-mode **5**, showed excellent abilities for highly syndiospecific polymerization of propene and 1-alkenes as well as copolymerization of ethene with higher 1-alkenes. We obtained a tetrahydrofuran (THF)-coordinated Ti analog **6**, which conducted copolymerization of ethene and dicyclopentadiene with high activity.[40] These results suggest the possibility of the isomerization of **4** during the polymerization, as shown in Scheme 7.[41] The PP obtained with **4** contained a considerable amount of mmmm and mmmr, suggesting the presence of isotactic blocks in the syndiotactic sequence. The isotactic block might be produced by the C_1-symmetric Ti species formed by the isomerization of **4**.

Table 12 Steric pentad distribution of PPs obtained by Ti complexes–dMMAO at 0 °C

	Stereopentad distribution[a]									
Ti	*mmm*	*mmmr*	*rmmr*	*mmrr*	*mmrm+rmrr*	*rmrm*	*rrrr*	*mrrr*	*mrrm*	T_m (*°C*)
1	0.00	0.00	0.04	0.09	0.10	0.04	0.60	0.13	0.00	89
2	0.00	0.00	0.04	0.08	0.05	0.02	0.69	0.12	0.00	92
3	0.00	0.00	0.02	0.03	0.02	0.00	0.86	0.07	0.00	142
4	0.02	0.05	0.03	0.08	0.16	0.05	0.45	0.15	0.01	—

[a]Determined by $_{13}$C NMR spectroscopy.

The diagnostic stereodefects in the syndiotactic sequence, 'rmmr' arising from the 'monomer miss-insertion' and 'rmrr' arising from the 'chain migration' without monomer insertion, are reduced as follows: rmmr, **1** (0.04)=**2** (0.04) > **4** (0.03) > **3** (0.02); and rmrr, **4** (0.16) > **1** (0.10) > **2** (0.05) > **3** (0.02). Thus, the high syndiospecificity of **3** can be ascribed to the reduced tendency for isomerization in addition to the high enantioselectivity.

The syndiospecific living polymerization of propene was also achieved by Fujita and colleagues[42,43] and Coates and colleagues[44] using bis(phenoxyimine)titanium derivatives activated with MAO. The active species of this catalyst is an octahedral Ti with a 2, 1-inserted propagation chain in which the chain-end chiral carbon

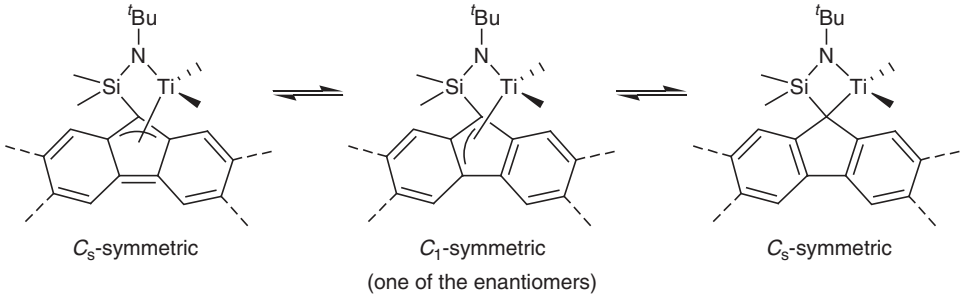

Scheme 7 Isomerization mechanism of **4**.

Table 13 Polymerization of higher 1-alkenes with 3–dMMAO at 0 °C[a]

Run	Monomer	Conv. (%)	Activity[b]	M_n [c] ($\times 10^4$)	M_w/M_n[c]	N[d] (μmol)	TOF[e] (s^{-1})	rr[f] (%)
42	1-Hexene	21	19200	49.3	1.27	0.64	98	88
43	1-Octene	13	15400	41.4	1.37	0.62	62	85
44	1-Decene	5	7800	26.6	1.55	0.50	32	86
45	1-Dodecene	5	9500	30.8	1.54	0.52	31	85

[a]Polymerization conditions: Ti=5 μmol, Al=4.0 mmol, higher 1-alkene=3.0 M, solvent=toluene, total volume=30 ml, time=1 min.
[b]Activity in kg-polymer mol-Ti^{-1} h^{-1}.
[c]Determined by SEC-MALS in THF.
[d]Number of polymer chains calculated from yield and M_n.
[e]TOF calculated from P_n and t_p.
[f]Determined by ^{13}C NMR spectroscopy.

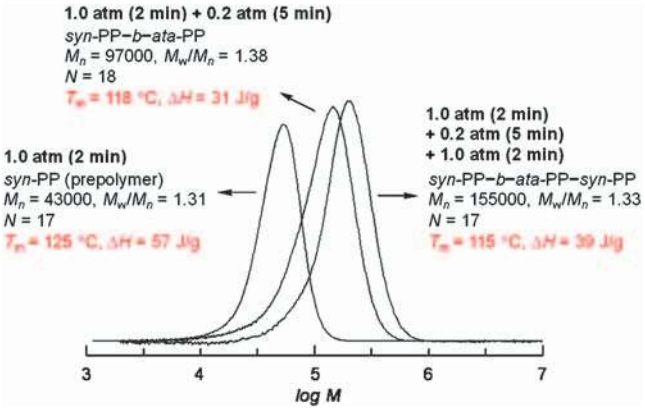

Figure 13 GPC curves of stereoblock PPs with **3**–dMMAO via propene pressure variation.[51]

isomerizes the chirality of the Ti species from one to the other in each monomer insertion to produce the syndiotactic polymers. Fujita and colleagues[45] succeeded in improving the syndiospecificity (rr=94%) by tuning the bis(phenoxyimine) ligand. The activity of propene polymerization with this catalytic system was significantly low, probably due to this stereospecific polymerization mechanism, as it conducted the living polymerization of ethene at a very high activity.[46]

One of the advantages in our syndiospecific living polymerization is the high propagation rate for propene polymerization. We therefore investigated the polymerization of a higher 1-alkene with **3**–dMMAO at 0 °C in toluene.[47] The results are summarized in Table 13. Although the activity was reduced as the length of 1-alkene was extended, an activity of 9500 kg-polymer·mol-Ti^{-1} h^{-1} was observed in 1-dodecene polymerization to produce a polymer with an M_n value of 308 000 after a 1-min polymerization. As the livingness of the system was confirmed by post-polymerization, the turnover frequency of each polymerization was determined from the M_n value evaluated by SEC-MALS, the molecular weight of the monomer and the polymerization time. The turnover frequency values obtained indicate that the propagation rate of 1-alkene decreased with δ the length of 1-alkene, but reached a definite value above that of 1-decene. Combined with the turnover frequency values of propene (26 s^{-1}) and 1-hexene (8 s^{-1}) obtained at different concentrations of the monomer and the catalyst, the relative reactivity of 1-alkene with **3**–dMMAO was determined as follows:

$$\text{propene}\,(3.3) > \text{1–hexene}\,(1.0) > \text{1–octene}\,(0.63) > \text{1–decene}\,(0.33) > \text{1–dodecene}\,(0.32)$$

The stereoregularity of the poly(1-alkene)s was syndiotactic with rr values of 85–88%, irrespective of the length of 1-alkene.

Synthesis of stereoblock PP

The syndiospecificity of the living *ansa*-dimethylsilylene(fluorenylamido)dimethyltitanium-based catalyst depends not only on the fluorenyl ligand but also on the polymerization conditions, such as solvent, temperature and monomer concentration, which enables us to synthesize tailor-made stereoblock copolymers composed of crystalline syndiotactic and amorphous PP sequences. Diblock copolymer was synthesized with **1**–dMMAO at 0 °C via propene polymerization in heptane (rr=72%), followed by post-polymerization after the addition of CB (rr=44%). The block copolymer (M_n=94 700, M_w/M_n=1.27) did not show any melting temperature (T_m) in the differential scanning calorimetry measurement, although the corresponding PP blend showed a T_m of 94 °C.[48] The use of **3** in place of **1** produced a crystallizable block copolymer: first polymerization in heptane, rr=89%, T_m=123 °C; second polymerization in heptane/CB, rr=50%; total, M_n=119 000, M_w/M_n=1.29, T_m=119 °C, rr=69%.[49] Diblock copolymer was also synthesized by inducing a temperature jump in toluene: first polymerization at −20 °C, rr=90%, T_m=123 °C, ΔH=69 J g^{-1}; second polymerization at 25 °C , rr=60%; total, M_n=101 000, M_w/M_n=1.32, T_m=121 °C, ΔH=30 J g^{-1}, rr=75%.[50] Diblock and triblock copolymers were synthesized via propene pressure variation, the GPC curves of which are shown in Figure 13.[51] The dependence of stereospecificity on propene pressure was reported by Shmulinson and Eisen[52] using a Ti benzaminate complex activated by MAO, where the stereospecificity was interconverted between being isospecific and non-stereospecific.

POLYMERIZATION OF NORBORNENE

Norbornene can be polymerized via three different mechanisms: a cationic mechanism, ring-opening metathesis and coordination insertion (vinyl-type addition). Among these mechanisms, the vinyl-type addition produces polynorbornene that possesses special properties, such as high thermal stability, high glass transition temperature (T_g), high transpar-

ency and low birefringence, because of its constrained saturated carbon skeleton. Such polymeric materials have created a higher demand on optical plastics in data storage and microelectronics technologies.

Coordination-insertion polymerization of norbornene was studied with $TiCl_4/R_3Al$ in the early 1960s, and a number of zirconocenes have been studied since the 1980s.[53,54] All of these catalysts, except for $(\eta^5\text{-}C_5H_5)Ti(OBz)_3$–MAO, have shown very low catalytic activity, and the products produced are insoluble in common organic solvents.

We have found that *ansa*-dimethylsilylene(fluorenylamido)dimethyltitanium **1**-based catalysts, which conduct living polymerization of 1-alkene, are also excellent catalysts for norbornene polymerization when combined with a suitable cocatalyst.[55,56] Table 14 shows the results of norbornene polymerization with **1** and **CGC-Ti** activated by dMAO in toluene. Complex **1** showed good activity above 20 °C to give polynorbornene with high molecular weights and narrow MWDs via coordination insertion. In contrast, **CGC-Ti** showed very poor activity under the same conditions to give a polymer that was insoluble in NMR (tetrachloroethane-d_2) and GPC (*o*-DCB) solvents, even at elevated temperature.

Table 14 Polymerization of norbornene with 1 and CGC-Ti using dMAO as cocatalyst at different temperatures[a]

Run	Catalyst	Temp. (°C)	Time (min)	Yield (g)	Activity[b]	M_n[c] ($\times 10^4$)	M_w/M_n[c]
46	**1**	0	120	1.44	36	18.7	1.48
47	**1**	20	5	1.81	1090	29.6	1.26
48	**1**	40	5	2.73	1640	24.0	1.13
49	**CGC-Ti**	0	120	trace	—	—	—
50	**CGC-Ti**	40	120	0.18	2.2	ND	ND

[a]Polymerization conditions: Ti=20 μmol, Al/Ti=400, [Norbornene]=1.2 M, solvent=toluene, total volume=30 ml.
[b]Activity=$kg_{(polymer)}$ mol-Ti^{-1} h^{-1}.
[c]Number-average molecular weight and molecular weight distributions were measured by GPC analysis using polystyrene standards.

Table 15 shows the effects of using a cocatalyst on norbornene polymerization with **1** in toluene at 20 °C. $Ph_3CB(C_6F_5)_4$ combined with Oct_3Al showed the highest activity (~5000 kg-polymer·mol-Ti^{-1} h^{-1}) among the cocatalysts employed. The conversion reached 95% within 2 min. MMAO and dMAO showed good activities (~1000 kg-polymer·mol-Ti^{-1} h^{-1}), but MAO showed very poor activity because of Me_3Al in MAO. All of the produced polymers possessed narrow MWDs, and the *N*/Ti values were below 1. It should be noted that MMAO gave the narrowest MWD of 1.07, which was most likely because of the good solubility of MMAO, indicating that dMMAO is not necessary for the living polymerization of norbornene with **1**. Chain transfer to R_3Al may be suppressed at the hindered propagation chain end during the norbornene polymerization process.

Table 15 Polymerization of norbornene with 1 using different cocatalysts[a]

Run	Cocatalyst	Time (min)	Activity[b]	Conv.[c] (%)	M_n[d] ($\times 10^4$)	M_w/M_n[d]	N/Ti[e]
47	dMAO	5	1090	56	29.6	1.26	0.30
51	MAO	5	56	3	0.55	1.26	0.90
52	MMAO	3	953	29	7.9	1.07	0.60
53	$Ph_3CB(C_6F_5)_4$+Oct_3Al[f]	2	4820	95	33.5	1.40	0.50
54	$Ph_3CB(C_6F_5)_4$+$^iBu_3Al$[f]	2	4280	85	20.2	1.41	0.70
55	$Ph_3CB(C_6F_5)_4$[g]	10	–	–	–	–	–

[a]Polymerization conditions: Ti=20 μmol, Al/Ti=400, [norbornene]=1.2 M, solvent=toluene, total vol.=30 ml., temperature=20 °C.
[b]Activity=kg-polymer mol-Ti^{-1} h^{-1}.
[c]Conversion was calculated from polymer yield.
[d]Number-average molecular weights and molecular weight distributions were measured by GPC using polystyrene standard.
[e]Molar ratio of number of polymer chain and **1**.
[f]B=20 μmol, R_3Al=400 μmol.
[g]B=20 μmol.

We have found that *ansa*-dimethylsilylene(fluorenylamido)dimethyltitanium **1**-based catalysts, which conduct living polymerization of 1-alkene, are also excellent catalysts for norbornene polymerization when combined with a suitable cocatalyst.[55,56] Table 14 shows the results of norbornene polymerization with **1** and **CGC-Ti** activated by dMAO in toluene. Complex **1** showed good activity above 20 °C to give polynorbornene with high molecular weights and narrow MWDs via coordination insertion. In contrast, **CGC-Ti** showed very poor activity under the same conditions to give a polymer that was insoluble in NMR (tetrachloroethane-d_2) and GPC (*o*-DCB) solvents, even at elevated temperature.

Table 15 shows the effects of using a cocatalyst on norbornene polymerization with **1** in toluene at 20 °C. $Ph_3CB(C_6F_5)_4$ combined with Oct_3Al showed the highest activity (~5000 kg-polymer·mol-Ti^{-1} h^{-1}) among the cocatalysts employed. The conversion reached 95% within 2 min. MMAO and dMAO showed good activities (~1000 kg-polymer·mol-Ti^{-1} h^{-1}), but MAO showed very poor activity because of Me_3Al in MAO. All of the produced polymers possessed narrow MWDs, and the *N*/Ti values were below 1. It should be noted that MMAO gave the narrowest MWD of 1.07, which was most likely because of the good solubility of MMAO, indicating that dMMAO is not necessary for the living polymerization of norbornene with **1**. Chain transfer to R_3Al may be suppressed at the hindered propagation chain end during the norbornene polymerization process.

The effects of the amount of MMAO on norbornene polymerization were investigated using **1** (Figure 14). Both the polymer yield and the M_n value linearly increased with the Al/Ti ratios and were accompanied by a narrowing of the MWD, which indicates that a large excess of MMAO is necessary to achieve a high propagation rate. The same phenomenon was observed in propene polymerization with **3**–dMMAO as described above. The narrow MWD of the produced polynorbornene, as compared with PP, may be ascribed to the fast initiation during norbornene polymerization.

The polynorbornenes obtained were amorphous, soluble in halogenated solvents and stable at temperatures up to 420 °C. A polynorbornene film was prepared by casting the polymer solution in CB. The transmittance of the film (thickness=54 μm) was 93% or higher in the range from 350 nm to 700 nm (Figure 15).

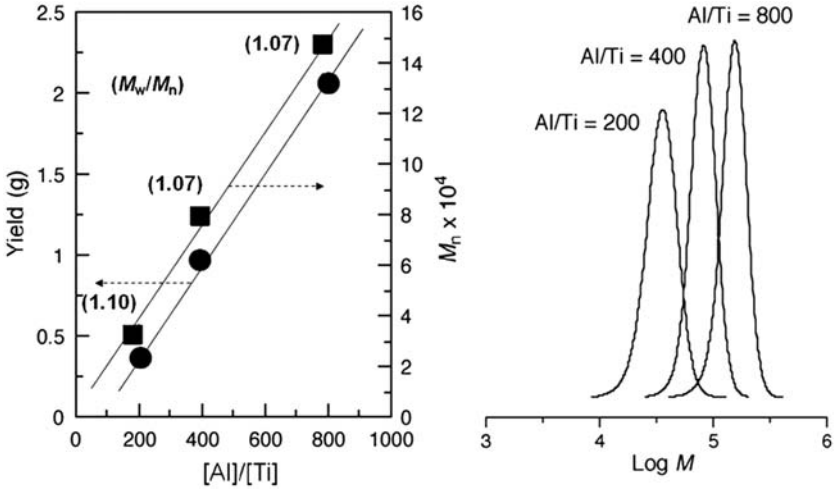

Figure 14 Effects of Al/Ti ratio on norbornene polymerization with **1**–MMAO. Polymerization conditions: Ti=20 μmol, dMMAO=8.0 mmol, solvent=30 ml, propene=1.26 g, temperature=0 °C, 1 h. Post-polymerization conditions: propene =1.26 g, 1 h.[56]

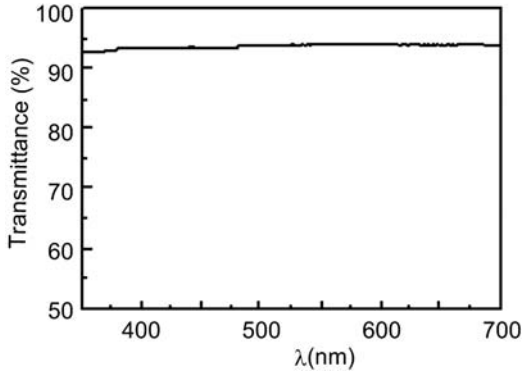

Figure 15 Transmittance of polynorbornene film (Run 52) in ultraviolet–visible region (350–700 nm).[56]

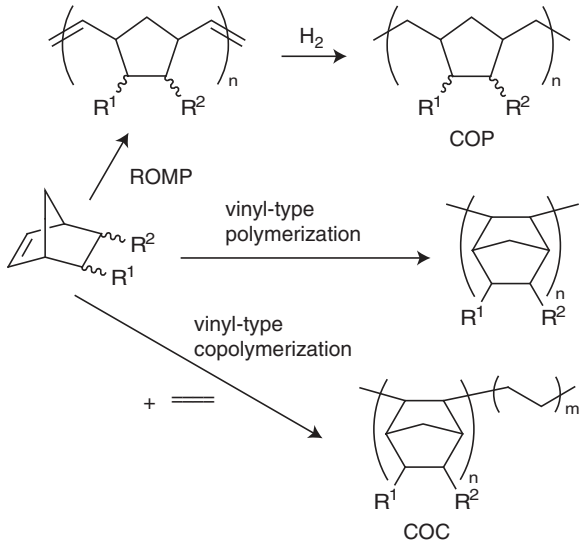

Scheme 8 Synthetic routes of cycloolefin polymer (COP) and cyclic olefin copolymer (COC).

COPOLYMERIZATION OF NORBORNENE WITH 1-ALKENE

Cycloolefin polymers and cyclic olefin copolymers, which consist of a rigid acyclic polymer backbone, are attractive materials because of their good heat and chemical resistance as well as their low dielectric constants, non-hygroscopicity and high transparency. Cycloolefin polymer is synthesized via ring-opening metathesis polymerization of norbornene derivatives followed by hydrogenation of C=C bonds along the main chain, whereas cyclic olefin copolymer is synthesized via the copolymerization of ethene and cycloolefins such as norbornene (Scheme 8).

One of the advantages of cyclic olefin copolymers is that their polymer properties can be easily controlled by the comonomer content and comonomer sequence. The development of early transition metal single-site catalysts enables us to synthesize poly(norbornene–*alt*–ethene) as well as poly(norbornene–*ran*–ethene), the T_g value of which can be controlled over a wide range.[57] A number of late transition metal-based catalysts have been reported to produce polynorbornene via coordination insertion with good activity, but they do not produce a copolymer with ethene because of the facile β-hydrogen transfer after ethene insertion.

Table 16 Copolymerization of ethene and norbornene with 1 and CGC-Ti activated by dMAO[a]

Run	*Ti*	*NB/E*	*Time (min)*	*Activity*[b]	M_n[c] ($\times 10^4$)	M_w/M_n[c]	*NB*[d] *(mol %)*	T_g[e] *(°C)*
56	**1**	2.5	1	520	6.3	1.63	35	88
57	**1**	5.0	2	1050	5.3	1.20	44	131
58	**1**	8.0	1	1650	6.1	1.35	50	156
59	**1**	10	1/4	2590	6.0	1.34	53	173
60	**1**	13	1/3	3250	6.3	1.32	58	185
61[f]	**1**	13	30	76	7.8	1.16	53	166
62	**CGC-Ti**	8.0	2	540	4.2	1.34	38	88
63	**CGC-Ti**	13	4	375	5.8	1.27	41	97
64	**CGC-Ti**	15	4	280	7.9	1.21	44	114

[a]Polymerization conditions: Ti=20 μmol, Al/Ti=400, solvent=toluene, total volume=50 ml, ethene=1 atm, temperature=40 °C.
[b]Activity=kg-polymer mol-Ti^{-1} h^{-1}.
[c]Molecular weights and molecular weight distributions were measured by GPC using polystyrene standards.
[d]Norbornene contents calculated from the ^{13}C NMR spectrum of copolymer.
[e]T_g was measured with differential scanning calorimetry.
[f]Temperature=0 °C.

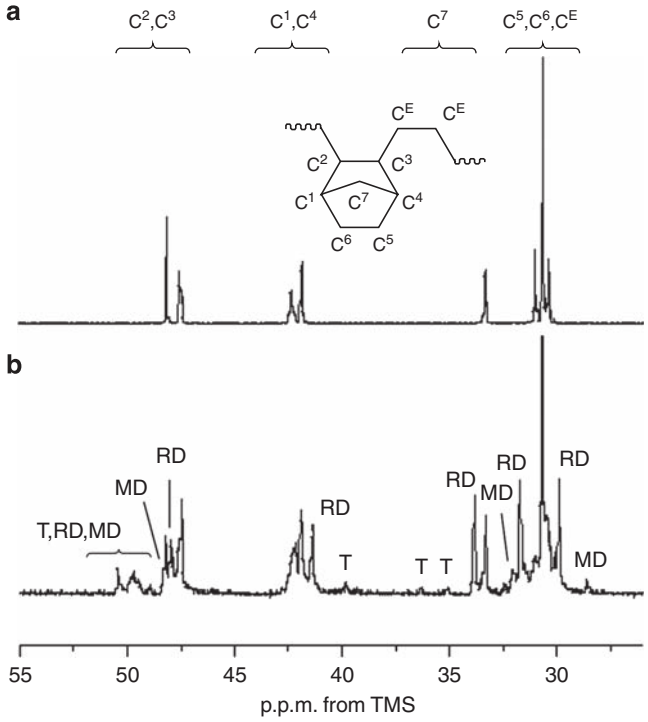

Figure 16 ^{13}C NMR spectra of ethene–norbornene copolymers obtained with (**a**) **CGC-Ti** and (**b**) **1** activated by dMAO. T, norbornene triad; RD, norbornene racemo dyad; MD, norbornene meso dyad.[54]

The other advantage of cyclic olefin copolymers is that their polymer properties can also be modified by the comonomer employed. However, the number of catalysts that copolymerize norbornene with propene or higher 1-alkene is very limited, and their activity and/or the molecular weight of the produced polymers is not sufficient.[58–63]

Ansa-dimethylsilylene(fluorenyl)(amido)dimethyltitanium-based catalysts were found to be active not only for 1-alkene polymerization but also for norbornene polymerization. We therefore applied these catalysts for copolymerization. We first conducted ethene–norbornene copolymerization with **1** and **CGC-Ti** activated by dMAO in toluene at

Table 17 Copolymerization of propene and norbornene with 1–dMAO[a]

Run	*N/P (mol/mol)*	*Time (min)*	*Activity[b] (g)*	M_n[c] *(×10⁴)*	M_w/M_n[c]	*NB[d] (mol %)*	T_g[e] *(°C)*
65	0.30	3	600	6.1	1.18	17	53
66	0.60	2	1580	9.5	1.11	36	112
67	1.13	7	866	13.8	1.14	58	198
68	2.00	12	895	15.6	1.16	71	249

[a]Polymerization conditions: Ti=20 μmol, Al/Ti=400, solvent=toluene, total volume=50 ml, propene=1 atm, temperature=20 °C.
[b]Activity=kg-polymer mol-Ti^{-1} h^{-1}.
[c]Molecular weight and molecular weight distributions were measured by GPC using polystyrene standards.
[d]Norbornene content calculated from the ^{13}C NMR spectrum of copolymer.
[e]T_g was measured with differential scanning calorimetry.

40 °C (Table 16).[64] Both complexes gave copolymers with high molecular weights and narrow MWDs. The activity of **CGC-Ti** was, however, one order of magnitude lower than that of **1**, and **CGC-Ti** required a high norbornene/ethene ratio in feed to incorporate norbornene in the copolymers compared with **1**.

The ^{13}C NMR spectra of the copolymers containing 44 mol% of norbornene are shown in Figure 16. The spectrum of the copolymer obtained with **CGC-Ti** shows only eight major resonances, which can be assigned to the alternating and the isolated norbornene sequences, as reported earlier by McKnight and Waymouth[65] for a series of *ansa*-dimethylsilylene(cyclopentadienylamido)dichlotitanium derivatives activated by MAO. The copolymer produced with **1** showed a completely different spectrum, indicating the presence of a norbornene dyad and triad.

Table 16 also shows the norbornene contents and the T_g values of the produced polymers determined by ^{13}C NMR and differential scanning calorimetry. The copolymers obtained by **1** showed higher T_g values than that obtained by **CGC-Ti** because of the norbornene–norbornene sequences as well as the high norbornene contents. The monomer reactivity ratios of the ethene–norbornene copolymerization with **1**–dMAO at 40 °C were determined to be r_E=5.6 and r_N,=0.08 by the Fineman–Ross method. The product of the reactivity ratios, $r_E r_N$=0.45, indicates the random nature of the copolymerization with **1**–dMAO. When the copolymerization was conducted at 0 °C, the MWD of the produced copolymer became narrow, 1.16, although the activity was significantly reduced (Run 61).[66]

The **1**–dMAO system also enabled the copolymerization of norbornene with propene to give high molecular weight copolymers with narrow MWDs (Table 17).[67] A typical ^{13}C NMR spectrum of the copolymer is illustrated in Figure 17, in which that of PP and polynorbornene obtained with the same catalyst are also shown as a reference. In the spectrum of the copolymer, the resonances assignable to the propene–norbornene sequence appeared. The comonomer contents were calculated from the relative intensity of the methyl groups with respect to the total carbons. The norbornene content was varied according to the norbornene/propene ratio in feed from 17 mol% to 71 mol%. Compared with the ethene copolymerization, low norbornene/comonomer ratio was sufficient to obtain a copolymer with a high norbornene content.

The T_g of the copolymer is plotted against the norbornene content of the copolymer in Figure 18, which gives a straight line. The results indicate that the T_g value of the copolymer should be freely controlled in the range of the T_g values of PP and polynorbornene.

The alkyl substituent on the fluorenyl group of **1** affected not only the activity but also the stereospecificity during propene polymerization, as described in the previous section. We therefore conducted propene–norbornene copolymerization with **1**–**4** activated by dMMAO (Table 18).[68] All of the complexes showed high activity during the copolymerization to produce copolymers with high molecular weights of 150 000–230 000 and narrow MWDs of 1.1–1.3

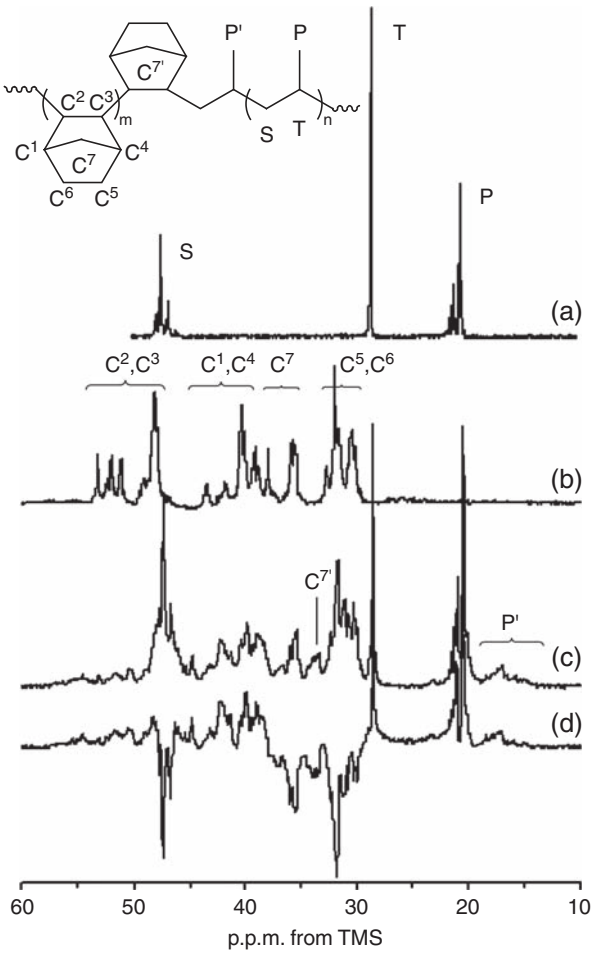

Figure 17 ^{13}C NMR spectra of (**a**) PP, (**b**) polynorbornene, (**c**) propene–norbornene copolymer and (**d**) DEPT 135 of the copolymer obtained with **1**–dMAO.[67]

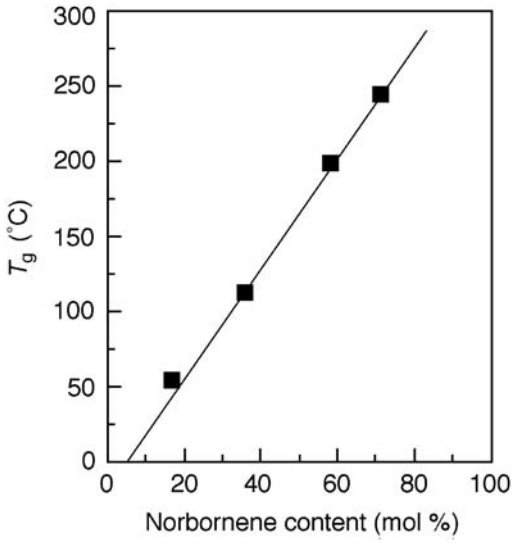

Figure 18 Plot of T_g versus norbornene content in the propene–norbornene copolymers.[67]

Table 18 Copolymerization of propene and norbornene with 1–, 2–, 3– and 4–dMMAO[a]

Run	*Ti*	*Al/Ti (mol/mol)*	*Time (min)*	*Activity*[b]	M_n[c] ($\times 10^4$)	M_w/M_n[c]	*NB*[d] *(mol%)*	*Conv.*[e] *(%)*	T_g[f] (°C)
69	**1**	400	3.0	1880	15.1	1.10	79	40	292
70	**2**	200	2.0	3000	16.7	1.14	81	43	291
71	**3**	200	1.0	4920	15.9	1.33	76	34	285
72	**4**	200	0.5	17100	23.2	1.30	71	57	250

[a]Polymerization conditions: Ti=20 μmol, propene=1 atm, norbornene=1.5 M, solvent=toluene, total volume=30 ml, temperature=20 °C.
[b]Activity in kg-polymer mol-Ti^{-1} h^{-1}.
[c]Molecular weights and molecular-weight distributions were measured by GPC using polystyrene standards.
[d]Norbornene contents in copolymer determined by ^{13}C NMR.
[e]Norbornene conversion calculated from yield and comonomer content.
[f]Glass transition temperatures determined by DSC.

Table 19 Copolymerization of norbornene and 1-octene with 1–, 2–, 3– and 4–dMMAO[a]

Run	*Catalyst*	*O/N*	*Activity*[b]	M_n[c] ($\times 10^4$)	M_w/M_n[c]	*NB*[d] *(mol%)*	*conv.*[e] *NB (%)*	*conv.*[e] *O (%)*	T_g[f] (°C)
73	**1**	1.5	340	5.3	1.19	80	22	4	213
74[g]	**1**	2	160	3.2	1.17	73	9	2	162
75	**2**	1.5	800	4.9	1.15	82	17	2	233
76[g]	**2**	2	520	3.4	1.15	74	9	2	176
77[g]	**3**	1.5	620	3.2	1.40	74	11	3	169
78[g]	**3**	2	700	4.0	1.35	68	11	3	153
79	**4**	1.5	1660	9.9	1.37	75	30	7	184
80	**4**	2	1660	6.5	1.46	67	27	7	143

[a]Polymerization conditions: Ti=20 μmol, Al/Ti=200, norbornene=0.7 M, solvent=toluene, total volume=33 ml, temperature=20 °C, time=5 min for **1** and 1.5 min for **2–4**.
[b]Activity in kg-polymer mol-Ti^{-1} h^{-1}.
[c]Molecular weight and molecular-weight distribution were measured by GPC using polystyrene standards.
[d]Norbornene content in copolymer determined by the ^{13}C NMR.
[e]Norbornene and 1-octene conversions calculated from yield and comonomer content.
[f]Determined by DSC.
[g]A different lot of dMMAO than that used in other entries.

in a few minutes. In propene polymerization, **4** gave polymers with broad MWDs. The narrow MWD of the copolymerization can partly be ascribed to the fast initiation reaction with norbornene. The dependence of the activity on the titanium complex was the same as that for propene polymerization: $\mathbf{4} \gg \mathbf{3} > \mathbf{2} > \mathbf{1}$. All of the catalytic systems gave amorphous copolymers with high norbornene contents (>70 mol%) and thus high T_g values (>250 °C).

The copolymerization activity of norbornene with propene was too high to maintain the norbornene conversion in low level, especially in the **4**–dMMAO system, which prevented the precise evaluation of the monomer reactivity ratios during copolymerization. In addition, there is no report on living copolymerization of norbornene with higher 1-alkene. We therefore conducted copolymerization of norbornene and 1-octene with **1**–**4** activated by dMMAO at various comonomer feed ratios. Some of the results are shown in Table 19.

Although the order of the activity of the titanium complexes was the same, the activity for the 1-octene copolymerization was one order of magnitude lower than that for propene copolymerization. It should be noted that **4**–dMMAO still exhibited a high activity of 1660 kg-polymer mol-Ti^{-1} h^{-1}. All of the catalytic systems gave high molecular weight polymers with narrow MWDs, although **3** and **4** gave slightly broader MWDs. The same tendency was observed in the propene copolymerization (Runs 71 and 72).

To confirm the living nature of the copolymerization with **4**–dMMAO, we conducted post-copolymerization, in which the same amount of norbornene–1-octene mixture was sequentially added after the first step copolymerization had been completed. The polymerization results and the GPC curves of the copolymers are shown in Figure 19, which implies that the copolymerization of norbornene and 1-octene with **4**–dMMAO proceeded in a living manner. The MWD in the post-copolymerization was narrower than that in the copolymerization (Runs 79 and 80 in Table 19), indicating that the broad MWD of the latter stems from the physical inhomogeneity caused by the high activity of the catalyst, namely the temperature distribution in the reactor because of the heat of polymerization and/or the ineffective stirring due to the produced polymers.

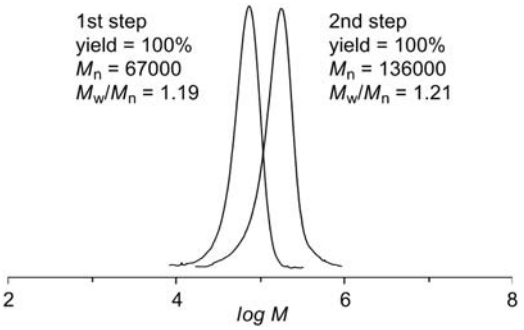

Figure 19 GPC curves of poly(norbornene-*co*-1-octene) obtained in post-polymerization with **4**–dMMAO at 20 °C.[68]

The ^{13}C NMR spectra of the copolymers containing ~75 mol% of norbornene obtained with each catalytic system are shown in Figure 20, which indicates the production of poly(norbornene–*co*–1-octene) in all of the catalytic systems. Although the detailed assignments of the resonances are not clear, the shapes of the spectra are slightly dependent on the titanium complex used. As each Ti complex possesses different stereospecificity in 1-alkene polymerization, the differences in the ^{13}C NMR spectra of the copolymers may be because of the differences in the stereoregularity of the copolymers.

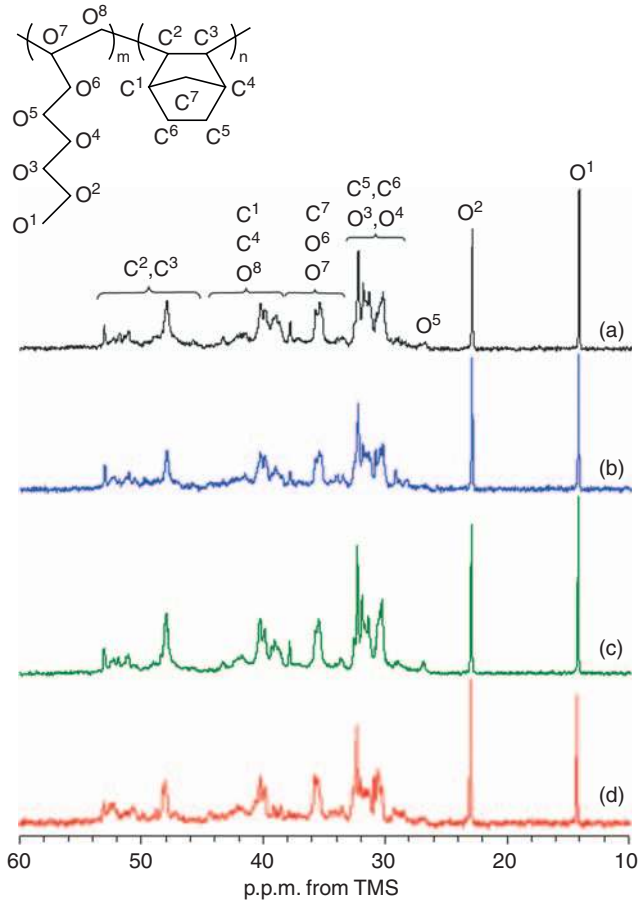

Figure 20 ^{13}C NMR spectra of poly(norbornene-*co*-1-octene) obtained with **1** (**a**) (75 mol%), **3** (**b**) (73 mol%), **2** (**c**) (74 mol%) and **4** (**d**) (75 mol%) with almost the same norbornene content.[68]

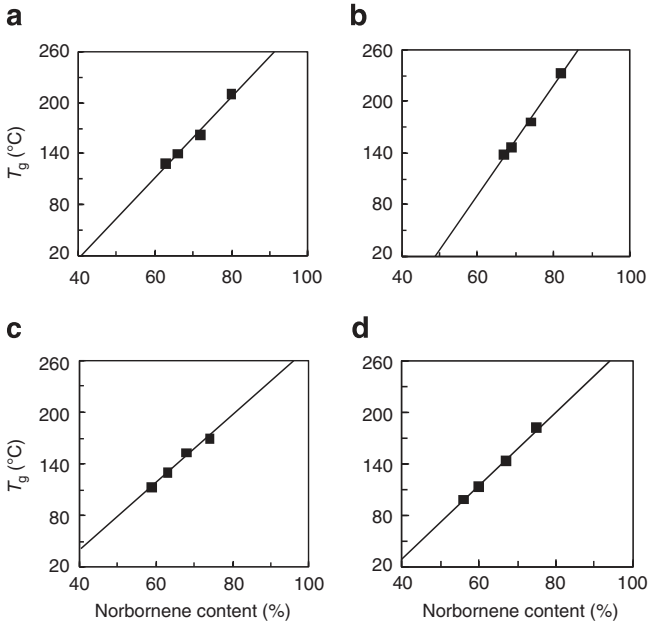

Figure 21 Plots of T_g value against norbornene content in poly(norbornene–*co*–1-octene) obtained with **1** (**a**), **2** (**b**), **3** (**c**) and **4** (**d**).[68]

Table 20 Monomer reactivity ratios of 1-octene-NB copolymerization with 1–4 activated by dMMAO[a]

Ti complex	r_{NB}	r_O	$r_{NB} \times r_O$
1	8.2	0.42	3.4
2	8.2	0.31	2.5
3	4.2	0.23	0.97
4	6.3	0.50	3.2

[a]Polymerization conditions: see the footnotes of Table 19.

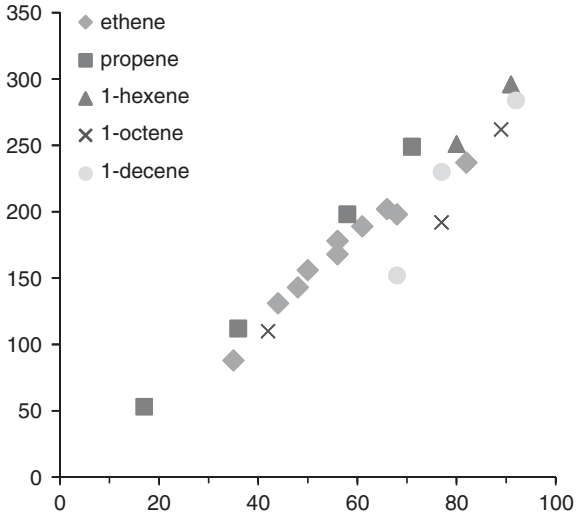

Figure 22 Plots of T_g versus norbornene content of poly(1-alkene–*co*–norbornene) obtained with **1**–$Ph_3CB(C_6F_5)_4$/Oct_3Al.[70]

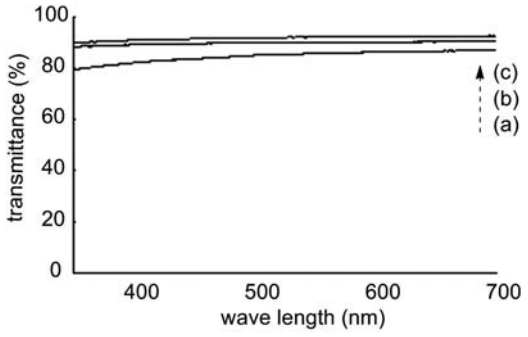

Figure 23 Transparency of poly(norbornene–*ran*–1-alkene) films: norbornene content, 92–93 mol%; film thickness, 120 μm. (**a**) 1-hexene, (**b**) 1-octene and (**c**) 1-decene.[70]

The T_g values of the copolymers, as determined by differential scanning calorimetry, are plotted against the norbornene content in Figure 21. The T_g value showed a linear relationship with the norbornene content in all of the catalytic systems, indicating the formation of uniform random copolymers regardless of the complex used. The slope of the straight line is, however, dependent on the titanium complex. The results also show that the microstructures of the copolymers are dependent on the complex used. Tritto and colleagues[69] reported that the stereoregularity of a norbornene sequence affected the T_g value of poly(norbornene-*co*-ethylene) with high norbornene contents.

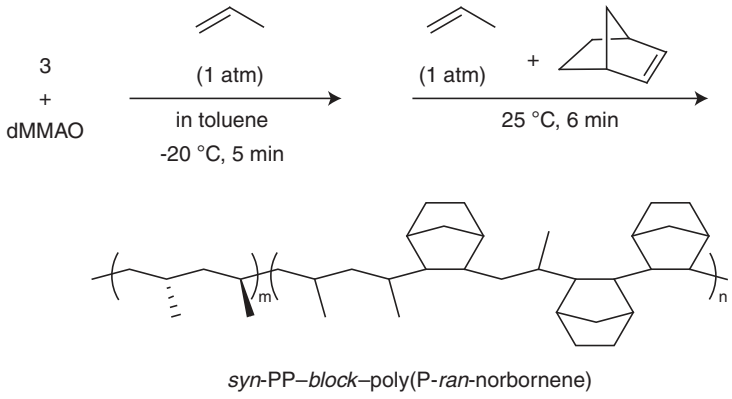

Scheme 9 Synthesis of block copolymer with **3**–dMMAO.

Table 21 Sythesis of *syn*–PP–*block*-poly(propene–*ran*–norbornene) with 3–dMMAO[a]

Run	*NB (g)*	*Time (min)*	*Yield (g)*	M_n[b] *(×10⁴)*	M_w/M_n[b]	T_m[c] *(°C)*	T_g[c] *(°C)*
(1.0 atm) — **3**, toluene, -20 °C, dMMAO → 25 °C							
Prepolymer[d]	0	0	0.48	10.8	1.36	135	—
81	2.77	6	0.92	20.8	1.21	135	311
82	2.07	6	1.12	22.4	1.30	133	231
83	1.38	6	1.09	22.6	1.32	133	93

[a]Conditions: toluene=30 ml, Ti=10 μmol, Al=2.0 mmol, propene=1 atm.
[b]Determined by GPC using polystyrene standards.
[c]Determined by DSC.
[d]Temperature=−20 °C, propene=1 atm, time=5 min.

The monomer reactivity ratios for each catalytic system were determined by the Fineman–Ross method, although the norbornene conversions were not maintained at a sufficiently low level, especially in the **4**–dMMAO system because of its high activity for norbornene. Table 20 shows the monomer reactivity ratios ($r_N=k_{NN}/k_{NO}$ and $r_O=k_{OO}/k_{ON}$) thus obtained. These values indicate a preference for the insertion of norbornene, regardless of the last inserted monomer unit. The product of the reactivity ratios ($r_Nr_O=0.97$) obtained with **3** indicates a tendency for the formation of a random copolymer, whereas the products of the reactivity ratios ($r_Nr_O=2.5\sim3.5$) obtained with **1**, **2** and **4** imply a preference for the formation of a homo-norbornene sequence in the copolymer.

We achieved highly active living copolymerization of norbornene and 1-alkene with the tetraalkyl substituted fluorenyl complex **4** activated by dMMAO. If one does not require livingness for copolymerization, the most simple complex **1** activated by $Ph_3CB(C_6F_5)_4$/Oct_3Al possesses a sufficient activity of 10^3 kg-polymer mol-Ti^{-1} h^{-1} for the copolymerization of norbornene with 1-alkenes to give random copolymers with M_n values of 70 000 ∼ 90 000 and M_w/M_n values of 1.4 ∼ 1.7. The T_g value of the copolymer was controlled over a wide range by the norbornene content, irrespective of the 1-alkene used (Figure 22).[70]

The molecular weights of the copolymers were sufficiently high to prepare self-standing films by the solution-casting method. The transparency of the films was found to improve according to the length of 1-alkene and reached ∼90% with poly(1-decene–*co*–norbornene) in the ultraviolet–visible region (Figure 23).

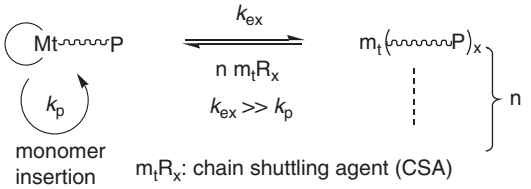

Scheme 10 Coordinative chain transfer polymerization.

SYNTHESIS OF OLEFIN BLOCK COPOLYMERS

The most important role of living polymerization is to synthesize block copolymers. It is therefore strongly encouraged to develop a living polymerization catalyst that is active for various monomers. the *ansa*-dimethylsilylene(fluorenylamido)dimethyltitanium derivatives **1**, **2** and **3** activated by dMAO or dMMAO were found to enable the living polymerization of propene and higher 1-alkene, where the rate of polymerization and the syndiotacticity of the produced polymers can be controlled by the Ti complex and/or the polymerization conditions, such as temperature, solvent and monomer concentration. The catalytic system has been also proven to conduct homopolymerization and copolymerization of norbornene with propene or 1-alkene in a living manner. Thus, we can synthesize any kind of block copolymer composed of 1-alkene and norbornene with this catalytic system.

As an example of the application of these living systems, we synthesized syndiotactic PP–*block*–poly(propene–*ran*–norbornene) with **3**–dMMAO according to the procedure shown in Scheme 9, and the results are summarized in Table 21.[49] The PP obtained in the first step showed an M_n value of 108 000 with an M_w/M_n of 1.36 and a melting point of 135 °C. After the copolymerization, the yields increased, as did M_n values (208 000–226 000); however, the M_w/M_n values decreased (1.21–1.32) regardless of the amount of norbornene added. The block copolymers showed T_m (133–135 °C) and T_g (93–311 °C) values that corresponded to that of the crystalline syndiotactic PP sequence and amorphous poly(propene–*ran*–norbornene) sequence, respectively, and the T_g values were controlled by the amount of norbornene added. These results suggest the formation of the expected block copolymers and the phase separation of the copolymers.

Although living polymerization is very useful for the synthesis of monodisperse polymers and tailor-made block copolymers, one catalyst molecule (initiator) is necessary for every polymer chain.

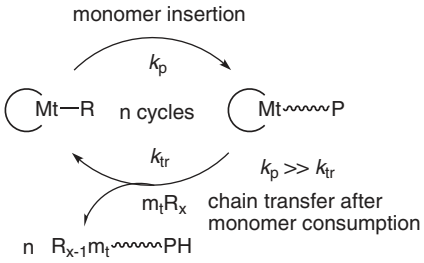

Scheme 11 Catalytic synthesis of monodisperse polymers with highly active living polymerization catalyst.

Table 22 Block copolymerization of norbornene and propene with 3 activated by dMMAO(1.8)[a]

Run	*Monomer*[b]	*Time (min)*	*Yield (g)*	*Conv.*	M_n[c] *(×10⁴)*	M_w/M_n[c]
84	NB	7	0.32	91	2.9	1.07
85	NB+P	7+30	0.98	100	12.8	1.13
86	NB+P+NB+P	7+30+7+30	1.96	100	12.9	1.18

[a]Polymerization conditions: dMMAO(1.8) containing 1.8 mol% of ^{i}Bu$_3$Al, toluene=30 ml, Ti=20 μmol, Al=4.0 mmol, temperature=20 °C.
[b]NB=norbornene (0.35 g); P=propene (0.63 g).
[c]Number-average molecular weights and molecular weight distributions determined by GPC using polystyrene standards.

The catalytic synthesis of monodisperse polyolefins has been achieved by the combination of a living polymerization catalyst and a large excess of main-group metal alkyls, such as R_2Zn and R_3Al, where the propagating polymer chain on the transition metal exchanges with the metal alkyls reversibly much faster than the propagation rate (Scheme 10). This kind of polymerization is referred to as coordinative chain transfer polymerization and the metal alkyls are referred to as chain-shuttling reagents.[71,72] A suitable combination of the catalysts, which differ in copolymerization ability, produced multiblock copolymers via the copolymerization of ethene with 1-octene in the presence of Et_2Zn as a chain-shuttling reagent. The synthesis of a multiblock copolymer through this mechanism is called chain-shuttling polymerization.[73] Ethene-based diblock copolymers were also synthesized by switching the monomer composition during coordinative chain transfer polymerization.[74]

The combination of a living polymerization catalyst and a suitable chain transfer reagent should give monodisperse polymers if the propagation rate is much faster than the chain transfer rate and chain transfer occurs only after all the monomer is consumed (Scheme 11). Mitani *et al.*[75] catalytically obtained monodisperse polyethene with an phenoxyimine-based (so-called FI) catalyst in the presence of a large excess of Et_2Zn by the sequential addition of the same amount of ethene. We proved this concept in propene polymerization with **3**–dMMAO by controlling the amount of ^{i}Bu$_3$Al in dMMAO.[76] The concept was applied in the catalytic synthesis of block copolymer as shown in Table 22.[77] Block copolymerization of norbornene and propene was conducted with **3** activated by dMMAO(1.8) containing 1.8 mol% of ^{i}Bu$_3$Al, in which propene was introduced before norbornene had been consumed (Run 85). Further sequential addition of norbornene and propene in the same manner did not change the M_n value or the narrow MWD (Run 86), indicating the catalytic synthesis of polynorbornene–*block*–poly(propene–*ran*–norbornene)–*block*–PP. We can conclude that the catalytic synthesis of block copolymers is possible by the sequential addition of monomers in a highly active living polymerization catalyst combined with a suitable kind and amount of chain transfer reagent (Scheme 12).

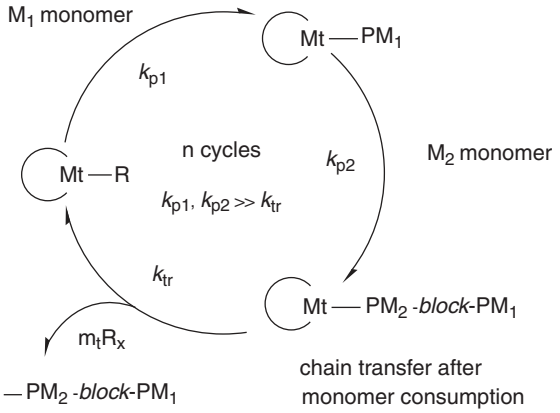

Scheme 12 Catalytic synthesis of monodisperse block polymers with highly active living polymerization catalyst.

CONCLUSIONS

1 and its derivatives activated by dMAO or dMMAO were found to conduct the living polymerization of propene at 0 °C and 25 °C. Solvent effects were investigated with **1** by using dMMAO, which is readily soluble in heptane. The syndiospecificity was improved by decreasing the polarity of the solvent from CB to heptane, accompanied by decrease in activity. The syndiospecificity and activity were also shown to be dependent on the alkyl substituent of the fluorenyl ligand. The activity monotonously increased with the number of introduced alkyl groups, whereas the highest syndiospecificity was obtained with the 3,6-^{i}Bu$_2$-substituted complex **3**. Thus, highly active and syndiospecific living polymerization of propene was achieved with **3**–dMMAO in heptane. The syndiospecificity of the catalysts also depended on the polymerization conditions, such as temperature or monomer concentration, a fact that was applied to the synthesis of stereoblock PPs. The catalytic system also conducted homopolymerization and copolymerization of norbornene and higher 1-alkene in a living manner with high activity in toluene. The **3**–dMMAO system was also proven to be catalytic in the synthesis of monodisperse block copolymers in the presence of a suitable amount of ^{i}Bu$_3$Al via selective chain transfer to ^{i}Bu$_3$Al after monomer consumption. These characteristics of the *ansa*-dimethysilylene(fluorenyl)(amido)dimethyltitanium-based catalysts can be applied to develop novel cycloolefin copolymers.

ACKNOWLEDGEMENTS

I acknowledge the coauthors of my paper quoted in this article for their experimental work and fruitful discussion, and the Tosoh Finechem Co. for donating cocatalysts.

1 Doi, Y., Ueki, S. & Keii, T. Living coordination polymerization of propene initiated by the soluble tris(acetylacetonato)vanadium-chlorodiethylaluminum system. *Macromolecules* **12,** 814–811 (1979).
2 Doi, Y. & Keii, T. Synthesis of 'living' polyolefins with soluble Ziegler-Natta catalysts and application to block copolymerization. *Adv. Polym. Sci.* **73–74,** 201–248 (1986).
3 Brintzinger, H. H., Fischer, D., Mülhaupt, R., Rieger, B. & Waymouth, R. M. Stereospecific olefin polymerization with chiral metallocene catalysts. *Angew. Chem., Int. Ed. Engl.* **34,** 1143–1170 (1995).
4 Kaminsky, W. New polymers by metallocene catalysis. *Macromol. Phys. Chem.* **197,** 3907–3945 (1996).

5 Britovsek, G. J. P., Gibson, V. C. & Wass, D. F. The search for new-generation olefin polymerization catalysts: life beyond metallocenes. *Angew. Chem. Int. Ed. Engl.* **38,** 428–447 (1999).
6 Coates, G. W. Precise control of polyolefin stereochemistry using single-site metal catalysts. *Chem. Rev.* **100,** 1223–1252 (2000).
7 Gibson, V. C. & Spitzmesser, S. K. Advances in non-metallocene olefin polymerization catalysis. *Chem. Rev.* **103,** 283–315 (2003).
8 Coates, G. W., Hustad, P. D. & Reinartz, S. Catalysts for the living insertion polymerization of alkenes: access to new polyolefin architectures using Ziegler-Natta chemistry. *Angew. Chem. Int. Ed. Engl.* **41,** 2236–2257 (2002).
9 As the best recent review. Edson, J. B., Domski, G. J., Rose, J. M., Bolig, A. D., Brookhart, M. & Coates, G. W. Living transition metal-catalyzed alkene polymerization: polyolefin synthesis and new polymer architectures. in *Controlled and Living Polymerizations* (eds Müller A. H. E & Matzjasyewski, K.) Ch. 4, 167–239 (Wiley-VCH: Weinheim, 2009).
10 Shapiro, P. J., Bunel, E., Schaefer, W. P. & Bercaw, J. E. Scandium complex [{(η^5-C_5Me_4)Me_2Si(η^1-$NCMe_3$)(PMe_3)ScH]$_2$: a unique example of a single-component a-olefin polymerization catalyst. *Organometallics* **9,** 867–869 (1990).
11 Okuda, J. Functionalized cyclopentadienyl ligands. IV. Synthesis and complexation of linked cyclopentadienyl-amido ligands. *Chem. Ber.* **123,** 1649–1651 (1990).
12 McKnight, A. L. & Waymouth, R. M. Group 4 *ansa*-cyclopentadienyl-amido catalysts for olefin polymerization. *Chem. Rev.* **98,** 2587–2598 (1998).
13 Hagihara, H., Shiono, T. & Ikeda, T. Syndiospecific polymerization of propene with [*t*-BuNSiMe_2Flu]TiMe_2-based catalysts by chain-end controlled mechanism. *Macromolecules* **30,** 4783–4785 (1997).
14 Resconi, L., Balboni, D. & Prini, G. Process for the preparation of metallocene compounds. *Application: WO Patent* **EP188,** 9936427 (1999).
15 Nishii, K., Hagihara, H., Ikeda, T., Akita, M. & Shiono, T. Stereospecific polymerization of propylene with group 4 *ansa*-fluorenylamidodimethyl complexes. *J. Organometal. Chem.* **691,** 193–201 (2006).
16 Cai, Z., Ikeda, T., Akita, M. & Shiono, T. Substituent effects of tert-butyl groups on fluorenyl ligand in syndiospecific living polymerization of propylene with ansa-fluorenylamidodimethyltitanium complex. *Macromolecules* **38,** 8135–8139 (2005).
17 Shiono, T., Harada, R., Cai, Z. & Nakayama, Y. A highly activecatalyst composed of *ansa*-fluorenylamidodimethyltitanium derivative for propene polymerization. *Top. Catal.* **52,** 675–680 (2009).
18 Nishii, K., Ikeda, T., Akita, M. & Shiono, T. Polymerization of propylene with [*t*-BuNSiMe_2Ind]TiMe_2-MAO catalyst systems. *J. Mol. Catal. A Chem.* **231,** 241–246 (2005).
19 Hagihara, H., Shiono, T. & Ikeda, T. Living polymerization of propene and 1-hexene with the [*t*-BuNSiMe_2Flu]TiMe_2/B(C_6F_5)$_3$ catalyst. *Macromolecules* **31,** 3184–3188 (1998).
20 Chen, E. Y.- X. & Marks, T. J. Cocatalysts for metal-catalyzed olefin polymerization: activators, activation processes, and structure-activity relationships. *Chem. Rev.* **100,** 1391–1434 (2000).
21 Shiono, T., Yoshida, S., Hagihara, H. & Ikeda, T. Kinetic features in living polymerization of propene with the [*t*-BuNSiMe_2Flu]TiMe_2/B(C_6F_5)$_3$ catalyst. in *Metal-organic Catalysts for Synthesis and Polymerization* (ed. W Kaminsky) Ch. 3, 264–273 (Springer-Verlag, Berlin Heidelberg, 1999).
22 Shiono, T., Yoshida, S., Hagihara, H. & Ikeda, T. Additive effects of trialkylaluminum on propene polymerization with (*t*-BuNSiMe_2Flu)TiMe_2-based catalysts. *Appl. Catal. A Gen.* **200,** 145–152 (2000).
23 Scollard, J. D. & McConville, D. H. Living polymerization of alpha -olefins by chelating diamide complexes of titanium. *J. Am. Chem. Soc.* **118,** 10008–10009 (1996).
24 Scollard, J. D., McConville, D. H. & Rettig, S. J. Living polymerization of α-olefins: catalyst precursor deactivation via the unexpected cleavage of a B-C_6F_5 bond. *Organometallics* **16,** 1810–1812 (1997).
25 Scollard, J. D., McConville, D. H., Payne, N. C. & Vittal, J. J. Polymerization of α-olefins by chelating diamide complexes of titanium. *Macromolecules* **29,** 5241–5243 (1996).
26 Hasan, T., Ioku, A., Nishii, K., Shiono, T. & Ikeda, T. Syndiospecific living polymerization of propene with [*t*-BuNSiMe_2Flu]TiMe_2 using MAO as cocatalyst. *Macromolecules* **34,** 3142–3145 (2001).
27 Ioku, A., Hasan, T., Shiono, T. & Ikeda, T. Effects of cocatalysts on propene polymerization with [*t*-BuNSiMe_2Flu]TiMe_2. *Macromol. Chem. Phys.* **203,** 748–755 (2002).
28 Hagimoto, H., Shiono, T. & Ikeda, T. Living polymerization of propene with a chelating diamide complex of titanium using dried methylaluminoxane. *Macromol. Rapid Commun.* **23,** 73–76 (2002).
29 Hagimoto, H., Shiono, T. & Ikeda, T. Supporting effects of methylaluminoxane on the living polymerization of propylene with a chelating (diamide)dimethyltitanium complex. *Macromol. Chem. Phys.* **205,** 19–26 (2004).
30 Nishii, K., Matsumae, T., Dare, E. O., Shiono, T. & Ikeda, T. Effect of solvents on living polymerization of propylene with [*t*-BuNSiMe_2Flu]TiMe_2-MMAO catalyst system. *Macromol. Chem. Phys.* **205,** 363–369 (2004).
31 Herfert, N. & Fink, G. Elementary processes in Ziegler catalysis. 5. Solvent effect on a stereospecific zirconocene/methylaluminoxane Ziegler catalyst. *Makromol. Chem.* **193,** 773–778 (1992).
32 McKnight, A. L., Masood, M. A., Waymouth, R. M. & Straus, D. A. Selectivity in propylene polymerization with group 4 Cp-amido catalysts. *Organometallics* **16,** 2879–2885 (1997).
33 Doi, Y., Suzuki, S. & Soga, K. A perfect initiator for 'living' coordination polymerization of propene: tris(2-methyl-1,3-butanedionato)vanadium/diethylaluminum chloride system. *Makromol. Chem. Rapid Commun.* **6,** 639–642 (1985).
34 Chen, M.- C. & Marks, T. J. Strong ion pairing effects on single-site olefin polymerization: mechanistic insights in syndiospecific propylene enchainment. *J. Am. Chem. Soc.* **123,** 11803–11804 (2001).
35 Busico, V., Cipullo, R., Cutillo, F., Vacatello, M. & Castelli, V. V. A. Metallocene-catalyzed propene polymerization: from microstructure to kinetics C_s-Symmetric *ansa*-Zirconocenes. *Macromolecules* **36,** 4258–4261 (2003).
36 Ewen, J. A., Jones, R. L., Razavi, A. & Ferrara, J. D. Syndiospecific propylene polymerizations with Group IVB metallocenes. *J. Am. Chem. Soc.* **110,** 6255–6256 (1988).
37 Miller, S. A. & Bercaw, J. E. Highly stereoregular syndiotactic polypropylene formation with metallocene catalysts via influence of distal ligand substituents. *Organometallics* **23,** 1777–1789 (2004).
38 Irwin, L. J. & Miller, S. A. Unprecedented syndioselectivity and syndiotactic polyolefin melting temperature: polypropylene and poly(4-methyl-1-pentene) from a highly active, sterically expanded η^1-fluorenyl- η^1-amido zirconium complex. *J. Am. Chem. Soc.* **127,** 9972–9973 (2005).
39 Irwin, L. J., Reibenspies, J. H. & Miller, S. A. A sterically expanded 'constrained geometry catalyst' for highly active olefin polymerization and copolymerization: an unyielding comonomer effect. *J. Am. Chem. Soc.* **126,** 16716–16717 (2004).
40 Nishii, K., Hayano, S., Tsunogae, Y., Cai, Z., Nakayama, Y. & Shiono, T. Highly active copolymerization of ethylene and dicyclopentadiene with [(η^1-t-BuN)SiMe_2 (η^1-$C_{29}H_{36}$)]TiMe_2(THF) complex. *Chem. Lett.* **37,** 590–591 (2008).
41 Alt, H. G. & Samuel, E. Fluorenyl complexes of zirconium and hafnium as catalysts for olefin polymerization. *Chem. Soc. Rev.* **27,** 323–329 (1998).
42 Saito, J., Mitani, M., Mohri, J., Ishii, S., Yoshida, Y., Matsugi, T., Kojoh, S., Kashiwa, N. & Fujita, T. Highly syndiospecific living polymerization of propylene using a titanium complex having two phenoxy-imine chelate ligands. *Chem. Lett.* **30,** 576–578 (2001).
43 Sakuma, A., Weiser, M.- S. & Fujita, T. Living olefin polymerization and block copolymer formation with FI catalysts. *Polym. J.* **39,** 193–207 (2007).
44 Tian, J., Hustad, P. D. & Coates, G. W. A new catalyst for highly syndiospecific living olefin polymerization: homopolymers and block copolymers from ethylene and propylene. *J. Am. Chem. Soc.* **123,** 5134–5135 (2001).
45 Mitani, M., Furuyama, R., Mohri, J.- I., Saito, J., Ishii, S., Terao, H., Kashiwa, N. & Fujita, T. Fluorine- and trimethylsilyl-containing phenoxy-imine Ti complex for highly syndiotactic living polypropylenes with extremely high melting temperatures. *J. Am. Chem. Soc.* **124,** 7888–7889 (2002).
46 Saito, J., Mitani, M., Mohri, J.- I., Yoshida, Y., Matsui, S., Ishii, S.- I., Kojoh, S.- I., Kashiwa, N. & Fujita, T. Living polymerization of ethylene with a titanium complex containing two phenoxy-imine chelate ligands. *Angew. Chem. Inter. Ed. Engl.* **40,** 2918–2920 (2001).
47 Cai, Z., Ohmagari, M., Nakayama, Y. & Shiono, T. Highly active syndiospecific living polymerization of higher 1-alkene with *ansa*-fluorenylamidodimethyltitanium complex. *Macromol. Rapid Commun.* **30,** 1812–1816 (2009).
48 Nishii, K., Shiono, T. & Ikeda, T. A novel synthetic procedure for stereoblock poly(propylene) with a living polymerization system. *Macromol. Rapid Commun.* **25,** 1029–1031 (2004).
49 Cai, Z., Nakayama, Y. & Shiono, T. Synthesis of crystallizable sydiotactic-atactic stereoblock polypropylene using a living polymerization system. *Kinet. Catal.* **47,** 274–277 (2006).
50 Cai, Z., Nakayama, Y. & Shiono, T. Synthesis of stereoblock polypropylene by change of temperature in living polymerization. *Macromol. Res.* **18,** 737–741 (2010).
51 Cai, Z., Nakayama, Y. & Shiono, T. Facile synthesis of tailor-made stereoblock polypropylenes via successive variation of monomer pressure. *Macromolecules* **41,** 6596–6598 (2008).
52 Shmulinson, M. & Eisen, M. Polypropylene polymerization—synthesis of elastomeric polypropylene. *J. Am. Chem. Soc.* **125,** 2179–2194 (2003).
53 Janiak, C. & Lassahn, P. G. The vinyl homopolymerization of norbornene. *Macromol. Rapid Commun.* **22,** 479–492 (2001).
54 Blank, F. & Janiak, C. Metal catalysts for the vinyl/addition polymerization of norbornene. *Coord. Chem. Rev.* **253,** 827–861 (2009).
55 Hasan, T., Nishii, K., Shiono, T. & Ikeda, T. Living polymerization of norbornene via vinyl addition with *ansa*-fluorenylamidodimethyltitanium complex. *Macromolecules* **35,** 8933–8935 (2002).
56 Hasan, T., Ikeda, T. & Shiono, T. Highly efficient Ti-based catalyst systems for vinyl addition polymerization of norbornene. *Macromolecules* **37,** 7432–7436 (2004).
57 Ma, R., Hou, Y., Gao, J. & Bao, F. Recent progress in the vinylic polymerization and copolymerization of norbornene catalyzed by transition metal catalysts. *Polym. Rev.* **49,** 249–287 (2009).
58 Henschke, O., Koller, F. & Arnold, M. Polyolefins with high glass transition temperatures. *Macromol. Rapid Commun.* **18,** 617–623 (1997).
59 Boggioni, L., Bertini, F., Zannoni, G., Tritto, I., Carbone, P., Ragazzi, M. & Ferro, D. R. Propene-norbornene copolymers: synthesis and analysis of polymer structure by ^{13}C NMR spectroscopy and ab initio chemical shift computations. *Macromolecules* **36,** 882–890 (2003).
60 Kaminsky, W., Derlin, S. & Hoff, M. Copolymerization of propylene and norbornene with different metallocene catalysts. *Polymer* **48,** 7271–7278 (2007).
61 Jung, H. Y., Hong, S.- D., Jung, M. W., Lee, H. & Park, Y.- W. Norbornene copolymerization with a-olefins using methylene-bridged *ansa*-zirconocene. *Polyhedron* **24,** 1269–1273 (2005).
62 Kaminsky, W., Hoff, M. & Derlin, S. Tailored branched polyolefins by metallocene catalysis. *Macromol. Chem. Phys.* **208,** 1341–1348 (2007).

63 Li, X., Nishiura, M., Mori, K., Mashiko, T. & Hou, Z. Cationic scandium aminobenzyl complexes. Synthesis, structure and unprecedented catalysis of copolymerization of 1-hexene and dicyclopentadiene. *Chem. Commun.* **28,** 4137–4139 (2007).
64 Hasan, T., Ikeda, T. & Shiono, T. Ethene-norbornene copolymer with high norbornene content produced by *ansa*-fluorenylamidodimethyltitanium complex using a suitable activator. *Macromolecules* **37,** 8503–8509 (2004).
65 McKnight, A. L. & Waymouth, R. M. Ethylene/norbornene copolymerizations with titanium CpA catalysts. *Macromolecules* **32,** 2816–2825 (1999).
66 Hasan, T., Shiono, T. & Ikeda, T. Living random copolymerization of ethene and norbornene using *ansa*-fluorenylamidodimethyltitanium complex. *Macromol. Symp.* **213,** 123–129 (2004).
67 Hasan, T., Ikeda, T. & Shiono, T. Random copolymerization of propene and norbornene with *ansa*-fluorenylamidodimethyltitanium-based catalysts. *Macromolecules* **38,** 1071–1074 (2005).
68 Cai, Z., Harada, R., Nakayama, Y. & Shiono, T. Highly active living random copolymerization of norbornene and 1-alkene with *ansa*-fluorenylamidodimethyl titanium derivative: substituent effects on fluorenyl ligand. *Macromolecules* **43,** 4527–4531 (2010).
69 Forsyth, J., Perena, J. M., Benavente, R., Perez, E., Tritto, I., Boggioni, L. & Brintzinger, H.- H. Influence of the polymer microstructure on the thermal properties of cycloolefin copolymers with high norbornene contents. *Macromol. Chem. Phys.* **202,** 614–620 (2001).
70 Shiono, T., Sugimoto, M., Hasan, T., Cai, Z. & Ikeda, T. Random copolymerization of norbornene with higher 1-alkene with *ansa*-fluorenylamidodimethyltitanium catalyst. *Macromolecules* **41,** 8292–8294 (2008).
71 Zhang, W. & Sita Lawrence, R. Highly efficient, living coordinative chain-transfer polymerization of propene with $ZnEt_2$: practical production of ultrahigh to very low molecular weight amorphous atactic polypropenes of extremely narrow polydispersity. *J. Am. Chem. Soc.* **130,** 442–443 (2008).
72 Zhang, W., Wei, J. & Sita, L. R. Living coordinative chain-transfer polymerization and copolymerization of ethene, α-olefins, and α,ω-nonconjugated dienes using dialkylzinc as 'surrogate' chain-growth sites. *Macromolecules* **41,** 7829–7833 (2008).
73 Arriola, D. J., Carnahan, E. M., Hustad, P. D., Kuhlman, R. L. & Wenzel, T. T. Catalytic production of olefin block copolymers via chain shuttling polymerization. *Science* **312,** 714–719 (2006).
74 Hustad, P. D., Kuhlman, R. L., Arriola, D. J., Carnahan, E. M. & Wenzel, T. T. Continuous production of ethylene-based diblock copolymers using coordinative chain transfer polymerization. *Macromolecules* **40,** 7061–7064 (2007).
75 Mitani, M., Mohri, J.-i., Furuyama, R., Ishii, S. & Fujita, T. Combination system of fluorine-containing phenoxy-imine Ti complex and chain transfer agent: a new methodology for multiple production of monodisperse polymers. *Chem. Lett.* **32,** 238–239 (2003).
76 Cai, Z., Shigemasa, M., Nakayama, Y. & Shiono, T. Catalytic synthesis of monodisperse polypropylene using a living polymerization system with *ansa*-fluorenylamidodimethyltitanium-based catalyst. *Macromolecules* **39,** 6321–6323 (2006).
77 Cai, Z., Nakayama, Y. & Shiono, T. Catalytic synthesis of a monodisperse olefin block copolymer using a living polymerization system. *Macromol. Rapid Commun.* **29,** 525–529 (2008).

Takeshi Shiono was born in Tokyo in 1958. He received Bachelor degree in Chemical Engineering and Master degree in Chemical Environmental Engineering from the Tokyo Institute of Technology in 1981 and 1983, respectively. He received his Ph. D. from the Tokyo Institute of Technology under the guidance of Professor Kazuo Soga in 1989. He started an academic career at the Chemical Resources Laboratory of the Tokyo Institute of Technology as an assistant professor in 1984 and was promoted to an associate professor in 1993. He was promoted to a full professor in Department of Applied Chemistry, Graduate School of Engineering, Hiroshima University in 2004. His research interests include design and application of coordination polymerization catalysis.